3-1-1995

DETECTING STATOR AND ROTOR WINDING FAULTS IN THREE-PHASE INDUCTION MACHINES

Jeffrey C. Robertson
Purdue University School of Electrical Engineering

Chee Mun Ong
Purdue University School of Electrical Engineering

DETECTING STATOR AND ROTOR WINDING FAULTS IN THREE-PHASE INDUCTION MACHINES

JEFFREY C. ROBERTSON
CHEE-MUN ONG

TR-EE 95-8
MARCH 1995

SCHOOL OF ELECTRICAL ENGINEERING
PURDUE UNIVERSITY
WEST LAFAYETTE, INDIANA 47907-1285

DETECTING STATOR AND ROTOR WINDING FAULTS IN THREE-PHASE INDUCTION MACHINES

Jeffrey C. Robertson

Professor Chee-Mun Ong

Purdue Electric Power Center

School of Electrical Engineering

Purdue University

1285 Electrical Engineering Building

West Lafayette, IN 47907-1285

March 1995

TABLE OF CONTENTS

Page

Page

LIST OF TABLES

Table Page

LIST OF FIGURES

Figure Page

Figure Page

ABSTRACT

Robertson, Jeffrey C. M.S.E.E., Purdue University, March 1995. Detecting Stator and Rotor Winding Faults in Three-Phase Induction Machines. Major F'rofessor: Chee-Mun Ong.

The purpose of this work is to investigate the efficiency of existing methods for on-line fault detection when applied to three-phase induction motors, specifically to test known theoretical calculations of harmonics developed by certain types of faults experimentally. The work involves the development of equipment and test procedures needed and research of existing methods of fault detection. The experiments are conducted by planting a fault in a test induction machine and then performing a Fast Fourier Transform (FFT) on the line current. The processed data are then compared with those from the same test machine before the fault was planted. Recognition of fault type is based on differences in spectra signatures on the line currents of the faulted and healthy machines. This method potentially may be applied to other types of machines.

CHAPTER 1. INTRODUCTION

In modern industrial facilities, thousands of electric motors work together in the manufacturing process. A great percentage of the applied motors are essential to the process. An unscheduled shutdown occurs if one of these motors were to fail. If it were possible to detect a developing fault, it would be possible to schedule an orderly shutdown of the complete process with more efficient utilization of material and labor. Because of the great expense associated with unscheduled downtime, it may be cost effective to continuously monitor the critical motors for certain incipient faults before one of these motors become inoperable.

A variety of faults can occur within three-phase induction motors during normal operation. Several, such as rotor cage malfunctions, rotor eccentricity or inter-turn insulation breakdown can result in a complete breakdown of the machine if the progress of the fault is not detected [1, 2, 3, 4, 5]. Condition monitoring techniques, developed to monitor the health of the motor, can be used to detect the onset of such fault conditions. These techniques are most useful if they can be implemented on-line along with a planned maintenance program to prevent unscheduled plant interruptions.

The machine parameters which are most often monitored include vibration, leakage flux, and line current. These three features are common in monitoring techniques used today. Line current is probably the most convenient of the three since in an industrial environment it is the most accessible parameter, can be measured remotely if needed, and requires simple instrumentation [2, 6]. The monitoring of line current forms the basis of the work presented in this paper.

1.1 Need for Further Research

As previously stated, there has been a variety of research conducted in motor condition monitoring and fault diagnostics. After researching the topic and discussing the problem, it was clear that the academic community has many different ideas and techniques for performing these tasks. The use of vibration techniques, leakage flux measurement, infrared thermography, line current measurement, and a host of other techniques, shows that this topic is very important in industry today.

Since industry is the main driver for such research, the decision was made to visit an industrial setting and find out what techniques are currently being used, the problems associated with these techniques, and to get ideas from industry representatives. Mr. Richard L. Stigall, Machine Repairman/World Transmission, Allison Transmission Division of General Motors agreed to a tour of the World Transmission facility and a personal interview. Mr. Stigall has been employed with General Motors since 1973, holds an M.E.T. Degree from Purdue University, and is certified by the Vibration Institute as a Level-One Vibration Analyst.

The tour and interview with Mr. Stigall was very interesting, providing further insight to the usage and requirements of condition monitoring equipment. The World Transmission division is primarily a machining and assembly facility. Internal shafts and gears are machine produced from slugs by mill, lathe, broach, and other machine operations. Once the components are produced they are heat treated, polished, and then transferred to other sections of the World Transmission facility for assembly. As can be seen by the types of operations performed, there are many different types of machines in this facility. Most of these machines have several motors, such as the main drive motors, lubricant pump motors, and cooling fan motors. As a rough estimate Mr. Stigall said they have approximately 1500 motors on approximately 230 different machines and that the majority of these motors are induction type motors.

Mr. Stigall is presently using vibration techniques to provide information on the health of the equipment in the World Transmission facility. Vibration analysis not only provides information on the motors in a system but can be used on gear boxes, pulley systems, and other mechanical components. There are problems associated with this type of condition monitoring. First, the vibration measured may be due to some other source and not to the motor being tested. This problem may be caused by a loose belt or mounting bolt, by bearing misalignment in the drive system (not in the motor), or by transmission from a neighboring machine operation. The technician testing the motor has to check several points, in several different positions, to make sure that the vibration signature is coming from the suspected motor. This means that the technician not only has to spend time diagnosing a problem but must have the proper training necessary to operate the equipment.

This raises the second problem of training. In Mr. Stigall's area there are eight machine repairmen on his shift. Two of these men are designated for predictive maintenance tasks such as vibration testing. Mr. Stigall is the only repairman trained to perform computer analysis on the vibration test data. With the large number of

machines and test points there is not enough time in a day to monitor every point in the plant on a regular basis. For this reason only critical motors and test points are monitored on a routine basis.

While someone like Mr. Stigall has both the expertise and the academic background to understand the complexity of the data analysis, most of the maintenance and repairmen in industry today are high school graduates with many years of hands-on experience. Expecting these people to understand how a spectrum analysis or fourier analysis of a data signal is performed would be too optimistic. With this in mind, the equipment needs to be designed for ease of operation. If a repairmen has to spend most of his time learning how to operate a piece of equipment or read the instructions every time he intends to use it, the equipment will not be used. Another idea is to allow one person to perform the data analysis and direct the other repairmen to perform the repairs. Mr. Stigall was very adamant in explaining how this does not work. Pin pointing the problem may take several trips to the machine with a vibration probe. Running a repairman back and forth is not only counterproductive but will soon have the repairman fighting against or completely ignoring the technique. In his opinion, the person making the diagnosis should also make the repairs. This technique enables the individual to see data correlation firsthand and speed the learning process.

Another problem with complex analysis techniques is the potential loss of man power. Once an employee has been trained to operate such sophisticated equipment the employee will be in a position to make a career advancement elsewhere. If the employee exercises this opportunity, the company not only loses man power but the time and capital it has invested in this employee.

Mr. Stigall also discussed the need for condition monitoring and fault detection techniques to meet manufacturing standards on a global basis. Such manufacturing standards as ISO-9000 require member corporations to maintain condition monitoring and vibration testing and to have personnel certified in the operation of this equipment. This certification process keeps unqualified individuals from performing consulting work and helps to regulate a level of industry competence.

1.2 Motivation

After completing the interview it was quite clear that more research needs to be performed in the condition monitoring and fault diagnostics area. As shown in the previous paragraphs, much is known by the academic community on the subject. As with most practical problems, the academic community is not the group who actually

have to use and repair factory equipment. The level of the present diagnostic tools is too complex and there is no easy way to cross check a fault diagnosis.

The objective of this thesis is to lay the foundation for further research in motor condition monitoring. It will examine the spectral information present in the line currents of motors with laboratory induced faults, cross-checking whatever signature components that may be produced against those present in unfaulted motors and predicted by expressions found in the literature. The purpose here is not just to validate those expressions but to obtain first hand experience on the types of problems associated with measurement, analysis, and diagnostics.

1.3 Outline of the Thesis

Chapter 2 begins with an examination of the known theoretical equations for calculating different types of induction motor fault harmonics. This chapter briefly discusses these fault harmonic equations and is not intended to provide a complete theoretical evaluation. A more thorough analysis of the fault harmonic equations may be found in the references provided in Chapter 2.

The experimental set up and related details are described in Chapter 3. The equipment used and procedures developed during the experiment are explained so that the reader will have a better understanding of why specific machines were chosen and how the laboratory equipment was operated. Section 3.2 discusses specific needs to properly analyze the acquired data with the FFT process.

In Chapter 4 the theoretical fault harmonics are tabulated to facilitate the discussion. The experimental results, in the form of FFT plots from the healthy and faulted machines are first compared to identify the harmonics caused by the fault. This is then compared to the tabulated information predicted from theoretical consideration. A brief discussion of each comparison is provided to point out areas of interest.

Chapter 5 contains the conclusions developed from this experiment, a discussion for the need for further research in the area of motor fault diagnostics, and suggestions for improving data gathering techniques are also discussed.

CHAPTER 2. THEORETICAL EVALUATION

2.1 Detection of Air-gap Eccentricity

Air-gap eccentricity can cause an induction machine to fail for a number of reasons. These may include shaft deflection, bearing wear, stator core movement, improper positioning of the rotor, and a host of others. This eccentricity will cause an unbalanced magnetic pull and if the eccentricity is large enough can cause rotor-to-stator rub. Damage can then occur to the rotor, the stator core, and stator windings. Air-gap eccentricity in the induction machine may be detected by non-invasive monitoring of the stator currents [1, 7] and is based on the following discussion.

Two types of air-gap eccentricities can be observed: static or dynamic in nature. Static eccentricity is a change of the radial air-gap along its length and is fixed in space. A non rotating eccentricity is another name for this type of eccentricity. This may be caused by improper positioning of the stator, ovality of the core, or by improper bearing alignment. Dynamic eccentricity is due to the center of the rotor not being at the center of rotation. The air-gap along the rotor length fluctuates as the rotor is being rotated and thus the name rotating eccentricity is applied. Dynamic eccentricities may be caused by a bent rotor shaft, worn bearings, and resonance at critical speeds.

Rotor movement in an induction motor is the result of electromagnetic interaction between the air-gap flux produced by the three-phase stator winding and the induced rotor currents. Radial magnetic forces are produced between the rotor and stator surfaces and are proportional to the flux density squared [3]. These forces result in stator core and winding vibration. As faults associated with rotor and stator windings and air-gap variations alter the normal air-gap flux waveform, quantities which are functions of the air-gap flux will also be affected. The magnetic flux waves in the air-gap are a function of the permeance and the magnetomotive force (m.m.f.). This means that the line current and stray flux signals can be used to monitor the condition of the motor. The analysis is based on the rotating wave approach [8].

It can be shown that the frequency components in the input current waveform of the induction machine, which are present due to air-gap eccentricity can be determined frorn Equation (2.1) [1, 3, 4, 7, 9].

$$f_e = f_1[(k \bullet Z_2 \pm n_d) \bullet (1 - s) / P \pm v] \quad ...(2.1)$$

Where f_e is the eccentricity frequency developed, f_1 is the fundamental stator frequency, k is any integer, Z_2 is the number of rotor slots, and n_d is the eccentricity order number. For static eccentricity n_d equals zero and for dynamic eccentricity n_d equals one. Also used in Equation (2.1) are, s, the slip developed by the machine, P, the number of pole-pairs, and v, the harmonic number of the stator m.m.f. time harmonics ($v = \pm 1, +3, \pm 5, +7, ...$). A full mathematical analysis may be found in Cameron, Thomson, and Dow [3, 4].

2.2 Detection of a Stator Winding Asymmetry

The two common types of stator faults that occur in induction machines are the grounded fault and the stator interturn short circuit. The most common method for detecting such stator faults is by detecting negative and zero sequence components in the stator currents [7]. The presence of sizeable negative or zero sequence currents may be used as an indication of a fault. Stator faults may also create the addition of air-gap flux harmonics which, at very high resolution, will be detectable in the stator current [1, 7, 9]. This flux is caused by the fact that when asymmetries exist in the magnetic or electric circuits of an imperfect machine, there is a net difference between the currents flowing in one part of an end winding as compared with the currents flowing in the other portion of an end winding which is diametrically opposite. Thus the net axial flux contains a harmonic component due to the fault and is directly related to the harmonic content of the stator currents.

Due to the presence of space harmonics, the air-gap flux density distribution of a symmetrical three-phase stator winding is not sinusoidal. The flux density distribution may be described by Equation (2.2) [1].

$$B(\theta,t) = B_1\cos(\omega_1 t - P\theta) + B_5\cos(\omega_1 t + 5P\theta) - B_7\cos(\omega_1 t - 7P\theta) + ... \quad ...(2.2)$$

In Equation (2.2), 8 is an angle around the periphery (θ=0 is along the a-phase axis of the stator), t is the time, P is the number of pole-pairs, and ω_1 is the angular stator supply frequency. It follows that even in a symmetrical three-phase machine, the induced rotor currents will have slip dependent frequencies due to the space harmonics. Furthermore, there are always small asymmetries present in every machine, these frequencies will

also be present in the axial leakage flux component due to the rotor currents. When these asymmetries are present, the air-gap flux density distribution will contain extra harmonics. These extra harmonics due to a stator voltage asymmetry may be found by evaluating Equation (2.3) [1].

$$f_s = f_1[v \bullet (1 \pm s) \pm (1)] \qquad ...(2.3)$$

The notation used in this equation is the same as those of Equation (2.1), except for v. For this equation v is defined as k / (P12) = 1, 3, 5, 7, etc., due to the normal winding configuration of the stator. Only fault harmonic frequencies falling on these values of v will appear in the current signal. A full mathematical derivation may be found in Vas [1] An interesting observation about this expression is that the number of stator slots in the induction machine does not play a role in the calculation of stator fault harmonic frequencies. Where as in Equation (2.1), the number of rotor slots present has a direct bearing on the fault harmonic frequency calculated. It is not known if the effects of the induction machine stator slots are zero or if the effects of the stator slots are just neglected.

2.3 Detection of a Rotor Asymmetry

The most commonly used electrical machines in industry today are the squirrel cage induction machines. This is mainly due to their reliability, robustness, and that they are inexpensive to manufacture. Squirrel cage machines with high power ratings are prefabricated and are manufactured with copper rotor bars and end-rings, while machines of lower power ratings are manufactured by using die-casting techniques. Manufacturing die-cast rotors can raise several problems, due to the fact that rotors must be free from asymmetries.

An asymmetry in the rotor cage will cause asymmetrical distribution of the rotor currents, and due to this, mechanical and thermal stresses on the cage can damage a rotor bar. Damage of one rotor bar can lead to the damage of surrounding bars, thus the damage can spread, leading to multiple bar fractures. In the case of a crack, the bar will overheat and cause the bar to break. The surrounding bars will carry higher currents and will also be subjected to larger thermal and mechanical stresses, thus being made more susceptible to cracking. Most of the current which would have flown in the broken bar will flow in the two bars adjacent to it. The large thermal stresses may also damage the rotor laminations. The temperature distribution across the rotor lamination is also

changed due to rotor asymmetry [1, 7]. Cracks in bars can be present at various locations, along the slot and at the end-ring-to-bar joints.

The presence of a rotor asymmetry affects the machines circuit in the same manner as the stator winding asymmetry. Therefore, the effects of a rotor asymmetry follows the earlier discussion and Equation (2.2). The fault harmonics associated with a rotor circuit asymmetry are given by Equation (2.4) [1, 7].

$$f_r = f_1 [v \bullet (1 - s) \pm s] \qquad ...(2.4)$$

The notation of this equation is the same as the previous fault equations. A full mathematical evaluation may be found in Vas [1]. As with Equation (2.3), the number of rotor bar slots are not taken into consideration in this fault harmonic frequency calculation. Also, in Equation (2.4), the number of broken rotor bars seems to not have an effect on the fault harmonic frequency calculation. This makes the application of Equation (2.4) simpler because finding the number of broken or damaged rotor bars may be impossible without dissecting the machine in question. Monitoring of working machines without having to take them off line for testing is an advantage.

CHAPTER 3. EXPERIMENTAL SET UP AND DETAILS

3.1 Experimental Set up and Components

The equipment used in this project was gathered with size and expense in mind. As can be seen in Figure 1, the test equipment and test motor can be placed on a table top in the laboratory. This provided ease of handling and allowed the use of equipment on hand. The completed laboratory set up included a PC based data acquisition system, with front-end signal conditioning, friction brake dynamometer, and three-phase induction motors. The complete experimental set up for this system is shown in Figure 2 and the experimental block diagram is Figure 3.

3.1.1 Data Acquisition System

Experimental data on the test motors were collected using a PC based data acquisition system. The PC used was equipped with a 486DX microprocessor and upgraded with eight megabytes of RAM. This allowed for processing of large data files at acceptable speeds.

A CIO-AD16JR-AT analog to digital conversion board manufactured by Computer Boards Inc. was used for digitizing the analog voltage and current waveforms. This board is mounted in one of the PC card slots, and has a capacity for eight differential-ended inputs at a given time. It gives 12 bits of resolution with a accuracy of 0.01% of the reading. It can sample up to a maximum frequency of 330 kHz, single channel.

To acquire the voltage and current waveforms, a simultaneous sample and hold board, CIO-SSH16 also manufactured by Computer Boards Inc., was used. This board can take in 16 differential inputs with an accuracy of ±1 bit. An LF398 sample and hold chip and an INA110 differential amplifier has been used on the board. The maximum aperture time is 250 ns and typical aperture uncertainty is quoted as 50 ns. The maximum acquisition time is 10 microseconds and the droop rate is ±100 μV/ms. The purpose of having this board is to be able to gather the two voltage and two current data lines simultaneously with minimum skew, so there would be little phase error between the two sets of data. At the front end of the SSH board are current and voltage isolation

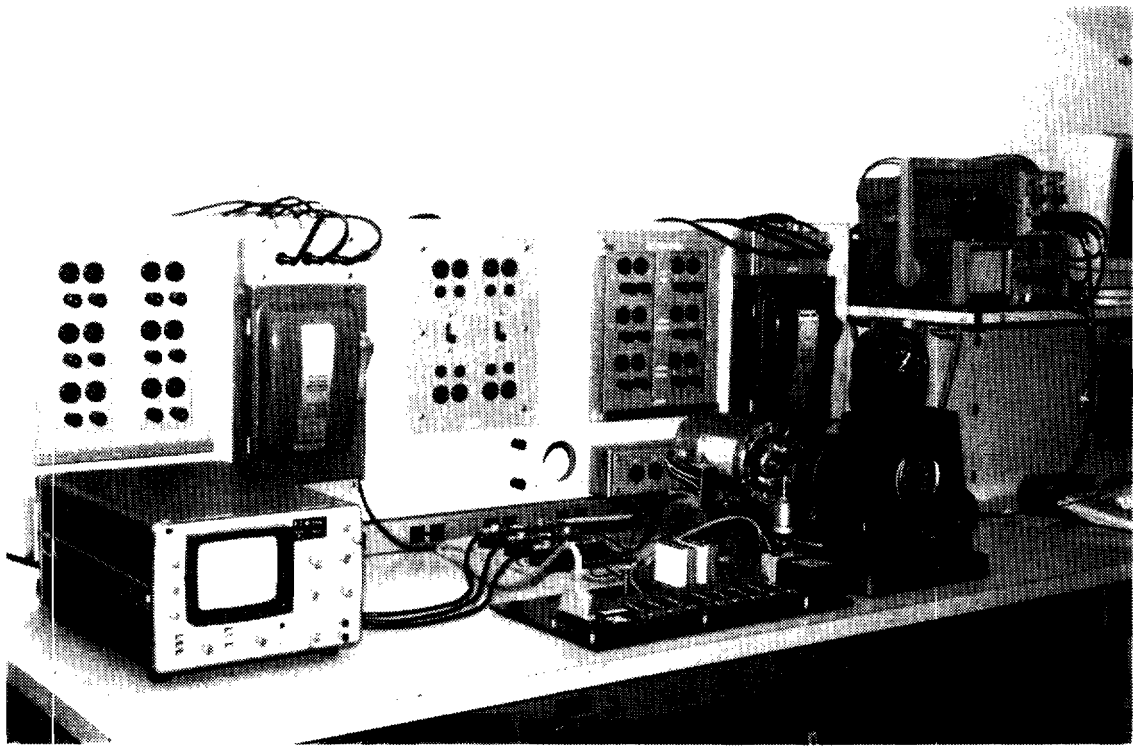

Figure 1 Close Up of Laboratory Equipment Set.Up

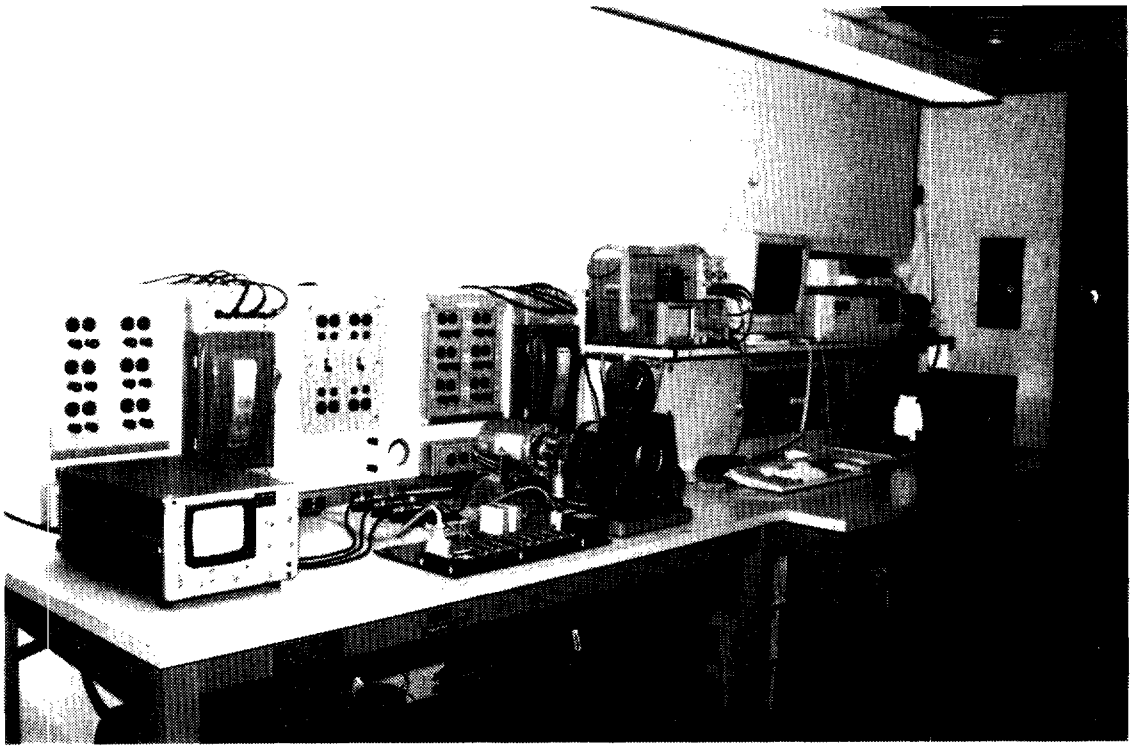

Figure 2 Complete Laboratory Set Up

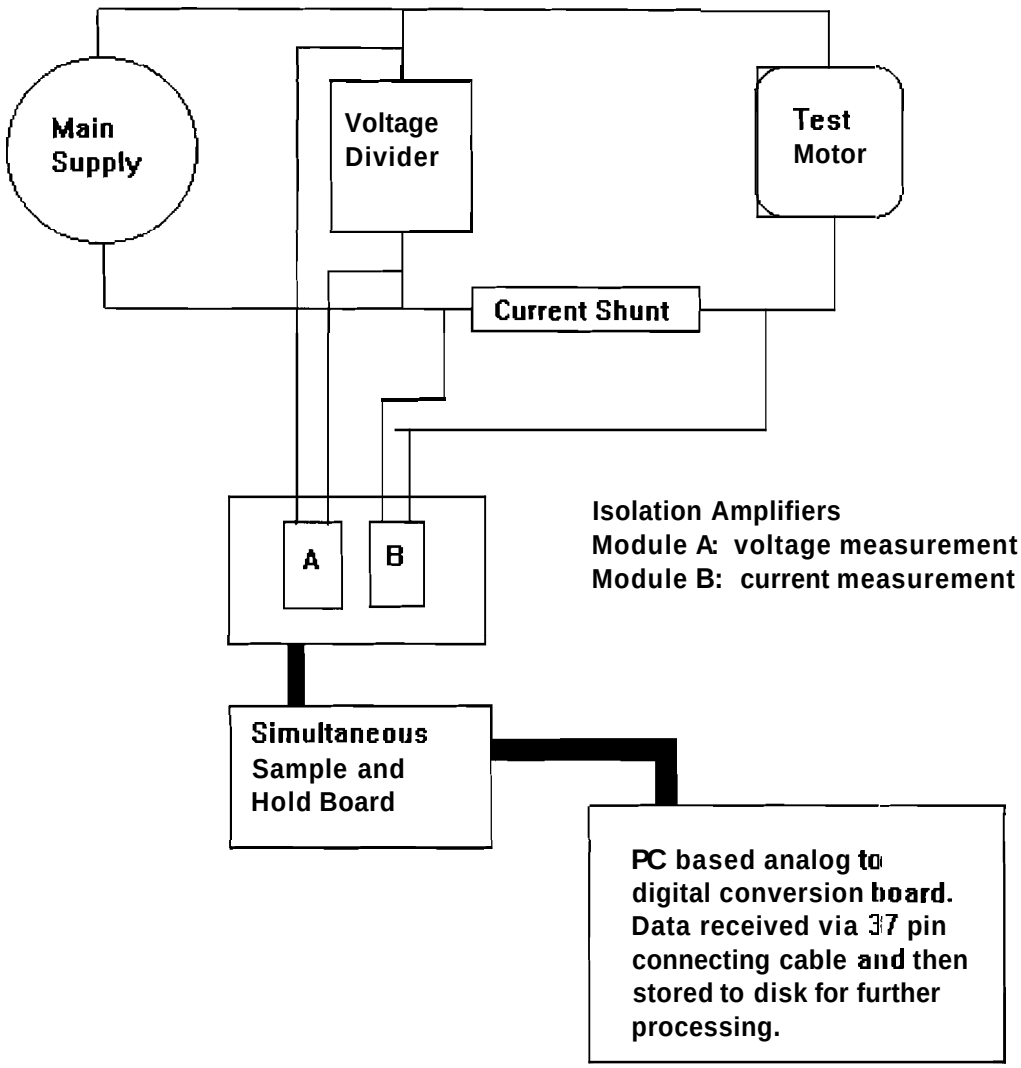

Figure 3. Laboratory Set Up Block Diagram

amplifiers, which provide electrical isolation between the power circuit under test and the PC based acquisition system. It was necessary to mount the amplifiers, so an ISO-RACK08 was used, again manufactured by Computer Boards Inc.. These amplifiers have adjustable gain ratios. The maximum input voltage level to the voltage amplifiers is 5 volts, and that to the current amplifiers is 50 mV. Figure 4 shows both the CIO-SSH16 and the ISO-RACK08.

Since the voltage and current amplifiers are not capable of handling the motor voltage and current directly, a shunt/divider board was built. HA-5-50 Bmpro shunts were used to obtain the proper input level to the current amplifier. A simple voltage divider, using one watt resistors, was designed for obtaining the proper input signal level to the voltage amplifiers. Figure 5 shows this board and how it was connected into the experimental set up.

3.1.2 Motor Analysis Dynamometer (MAD)

The MAD used in the laboratory proved to be a very vital piece of equipment for this experiment by providing an adjustable braking load to the motor. A digital tachometer was added for a more accurate measurement of the motor speed during testing. Figure 6 and Figure 7 show the MAD and mounted tachometer. As can be seen in the previous pictures, the MAD also provided a dial reading of the braking torque in foot-pounds. The horsepower developed could be calculated from the speed and torque measurements. The MAD was found stored in the sub-basement of the Electrical Engineering building and was in very poor condition. Several new parts had to be produced in the student machine shop. The MAD was reassembled and calibrated using data provided by the manufacturer.

3.2 Analysis of Acquired Data

The acquired data is stored on the hard disk of the PC, from which it can be retrieved for later processing. The processing involved several different routines each written for a specific task. The first task is to sort the data from the five input channels into separate files. The Fast Fourier Transform (FFT) is then used to find the magnitude and phase of the harmonic components in the current and voltage waveforms. The output from the FFT is then scanned to determine if frequency components that characterize a particular fault type are present.

In recovering the correct information from the FFT it is important to understand what is involved in an FFT analysis. This information may be found in any good signal

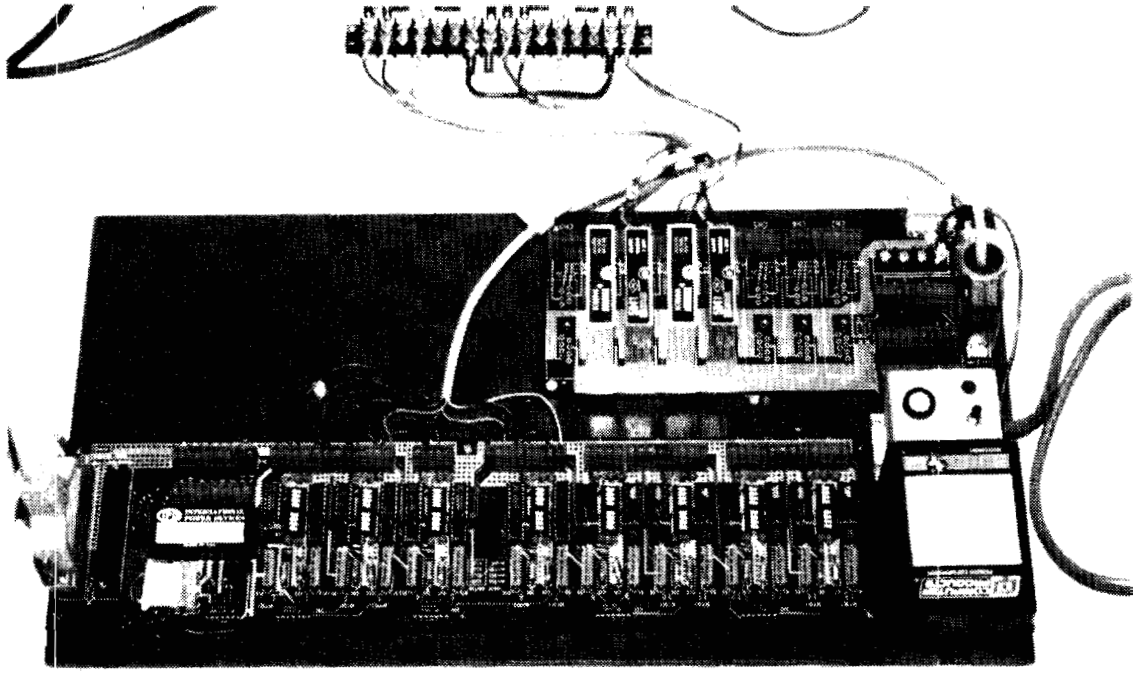

Figure 4 CIO-SSH16 and ISO-RACK08 Boards

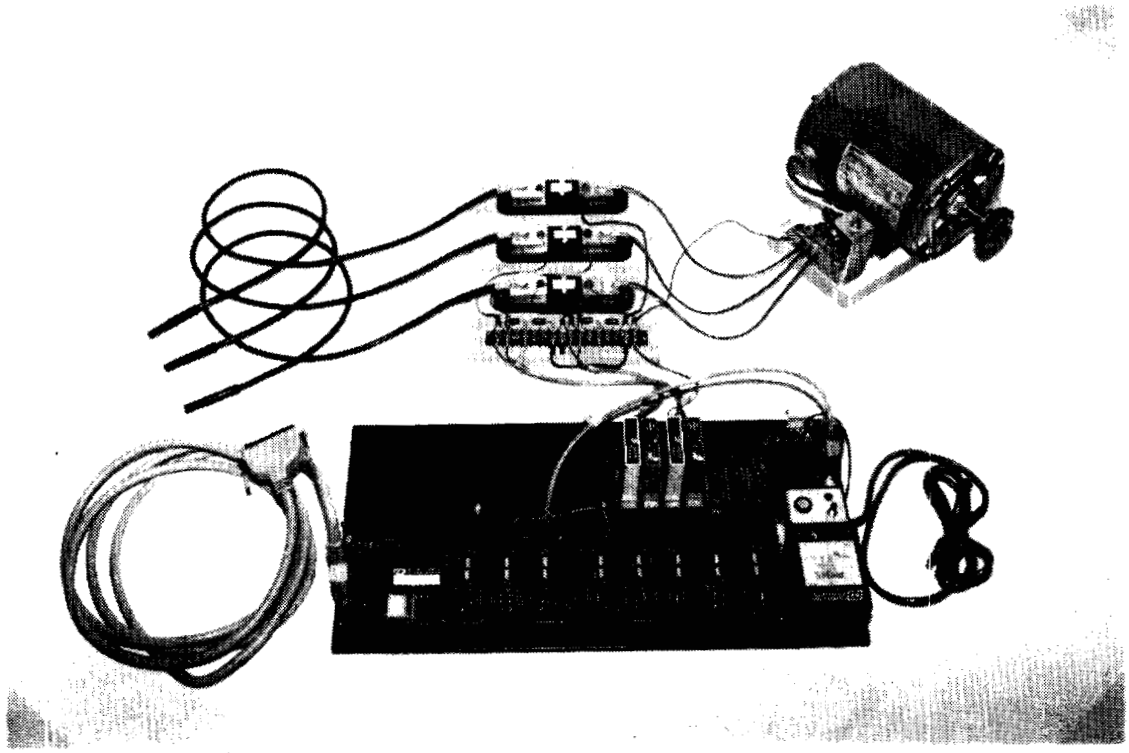

Figure 5 Shunt/divider Board Connected to System

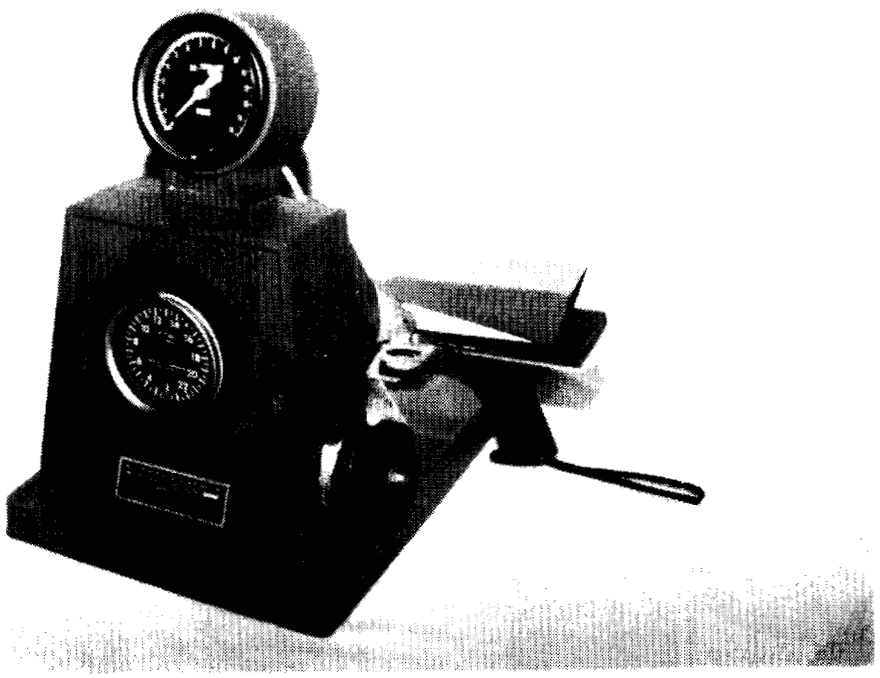

Figure 6 Front View of Motor Analysis Dynamometer (MAD)

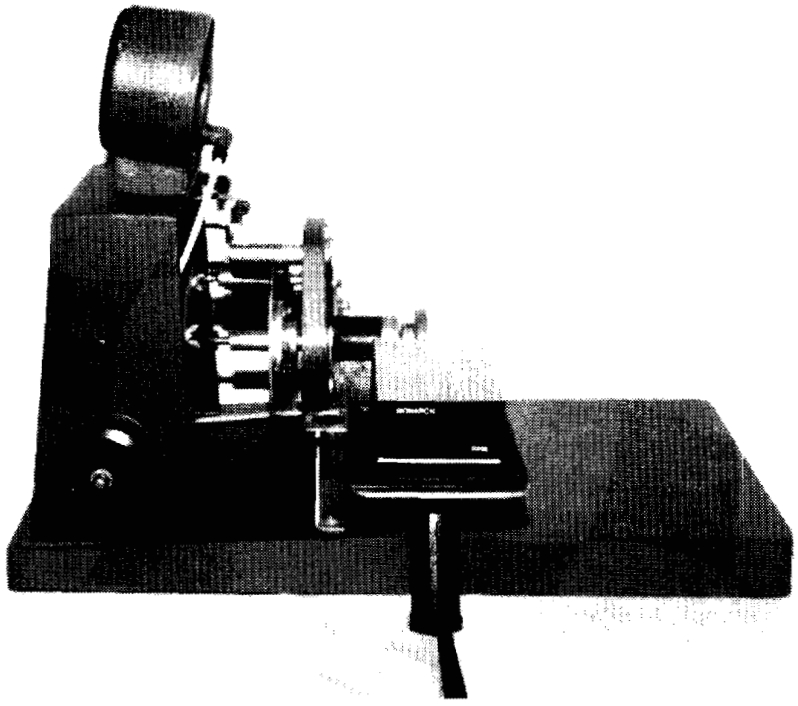

Figure 7 Side View of MAD Showing Electronic Tachometer

pracessing text [10]. In particular, errors from spectral leakage and picket fencing effect could affect the accuracy of the data under test. There are certain ways to reduce these errors which should be adhered to while using the FFT analysis software. One important consideration is the number of cycles of data on which the FFT is applied. To minimize the spectral leakage and picket fence effects the number of data cycles should be integral. The effect of not having an integral number is that the harmonic peaks will not fall on frequencies which are exact multiples of the fundamental. Such a situation will give incorrect magnitude and phase angles of the data under test. This problem may be avoided simply by truncating the data within a time window in which the data starts at a specific point on the cycle and ends an integral number of cycles later at the corresponding point. Performing this task on both the start and end of the data files created a very clean and accurate FFT output. Figure 8 and Figure 9 shows the raw data and the windowed data respectively.

Another important consideration involved in the FFT is the speed of the acquisition system. The sampling frequency has to be held at a rate fast enough to avoid aliasing. If the sampling rate is not fast enough then aliasing will distort the FFT output. The limiting factor is the speed of the equipment. In this experiment five channels were sampled simultaneously with a sample and hold amplifier in each channel to minimize skewing between these channels. The maximum sampling rate that could be performed is divided by five. This reduces the per channel rate down. If the per channel rate is not fast enough distortions in the FFT output can render it useless for identifying certain harmonics of interest.

The sampling frequency also plays a role in displaying an FFT. Equation (3.1) shows how the bin number, sampling frequency, and the number of samples (of the trimmed data file) are used to show the relationship between the bin number and the actual frequency.

$$f = (\text{bin number} - 1) \bullet f_s/N \qquad \ldots (3.1)$$

It is important to know that for this equation to be accurate the ratio of sampling frequency to the number of samples has to be a whole number or one-half a whole number. If this criteria is not fulfilled, the FFT output at discrete frequency when fitted over by a curve will give an appearance of a frequency shift. With this in mind, there is a need to calculate a proper sampling frequency that will allow the trimming of the data file to produce an integral number of cycles, allow the sampling frequency divided by

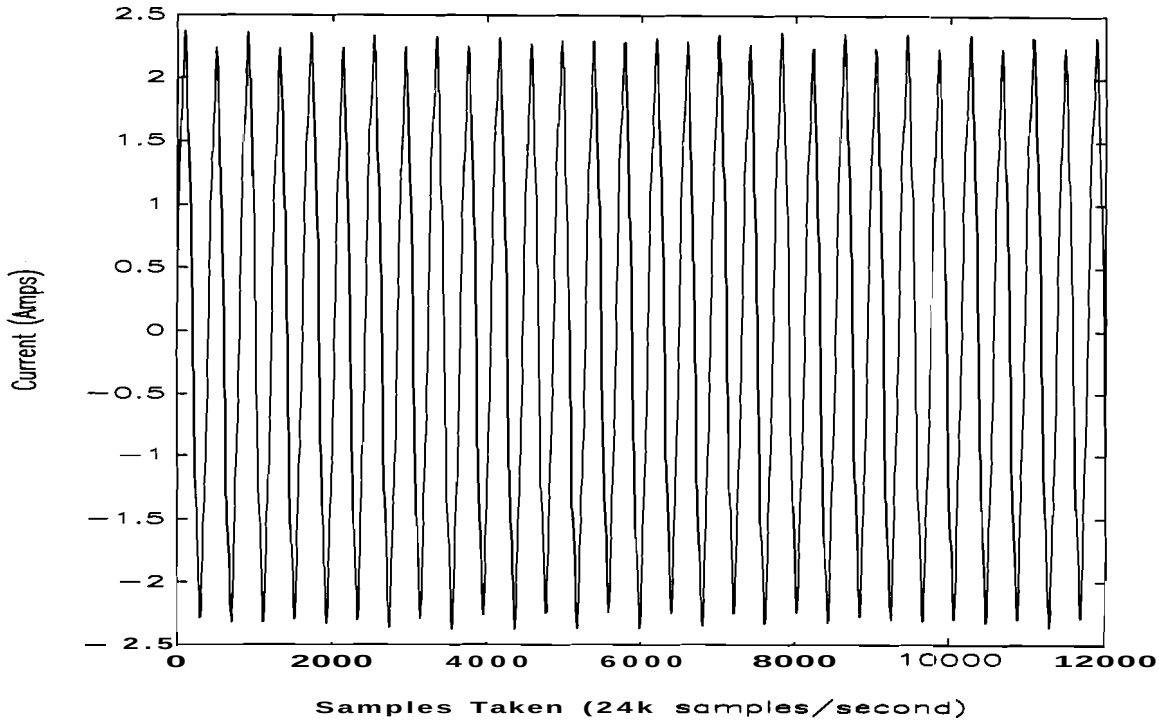

Figure 8 Raw Data of Current Waveform

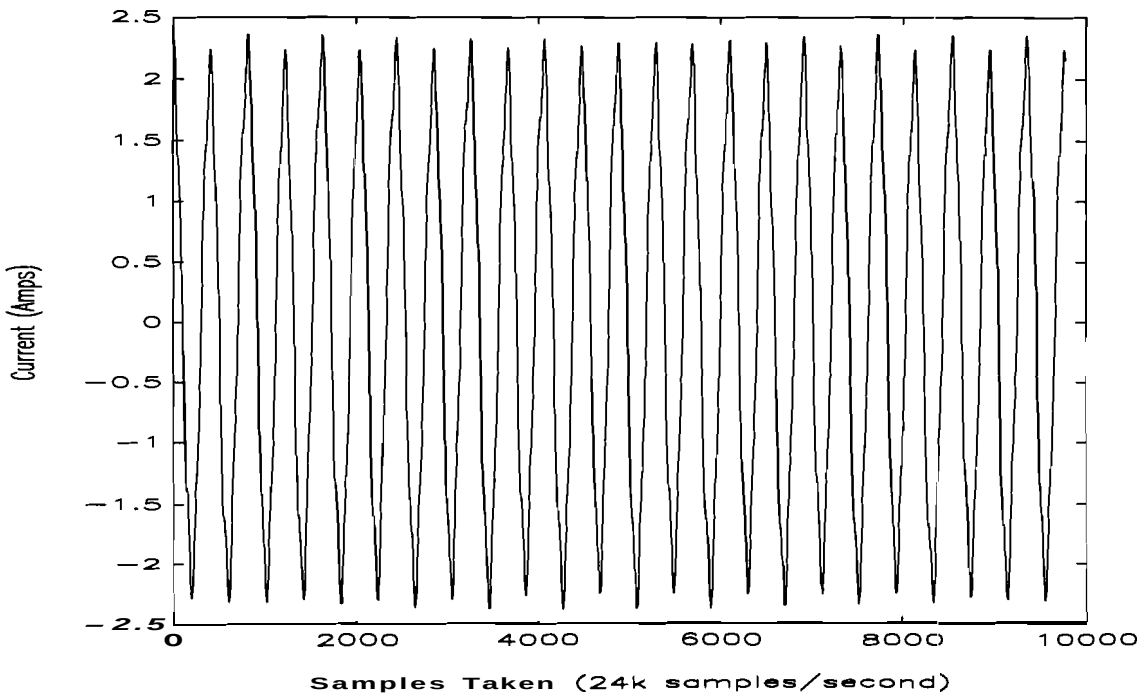

Figure 9 Windowed Current Data

the number of samples to be a whole number or one-half of a whole number, and be fast enough to provide the accuracy needed to display all harmonics (i.e. meets Nyquist criteria). If all the above criteria are fulfilled then the FFT analysis on a given signal will be very accurate.

3.3 Motor Preparation and Fault Planting

The three-phase induction motor was chosen because it is the industry workhorse, ranging from a few horsepower to thousands of horsepower. The first phase of the experiment was to determine the characteristics of all four test machines. This would set a base line for all four machines and also identify any initial dissimilarities between them. All test machines were mounted on Plexiglas blocks which allowed proper alignment with the MAD input shaft and isolated the test motors from the laboratory equipment. Figure 10 shows the test motor on the Plexiglas rnounting and Figure 11 shows the complete motor assembly with the MAD. After the bench marking tests, faults were deliberately planted. For this study, we investigated three kinds of common faults: rotor static eccentricity due to uneven bearing wear, shorted and open turns on a stator phase winding, and open rotor winding due to cracks in a rotor bar. The: findings of these tests will be discussed in later chapters.

3.3.1 Adjustable Bearing Carrier

The rotor eccentricity experiment was carried out by using an adjustable rotor bearing carrier. This adjustable carrier was manufactured in the student machine shop. It consists of an aluminum housing with a bearing block that has been mounted on a brass adjusting rod. Figure 12 and Figure 13 show the inside and outside of the carrier. As can be seen in Figure 13, locking nuts were placed on both sides of the vertical plates. This allowed the rod to be locked in position and held at very close tolerances when adjusting the rotor shaft. Figure 14 shows how the machine frame was modified so that a micrometer depth gauge could be used to measure the exact position of the shaft. Figure 15 shows the gauge used. Using the depth gauge allowed one end of the rotor to be moved to within 0.001 of an inch from the stator bore, thus providing the best results in this experiment. Since the air-gap of the test machine was so small, only one end of the rotor needed to be adjusted to produce this fault. Figure 16 and Figure 17 show the completely assembled machine. Having an adjustable bearing carrier allowed the rotor to be moved and then realigned, so that calibration checks and initial trials of sampling frequencies could be performed without permanently damaging the machine.

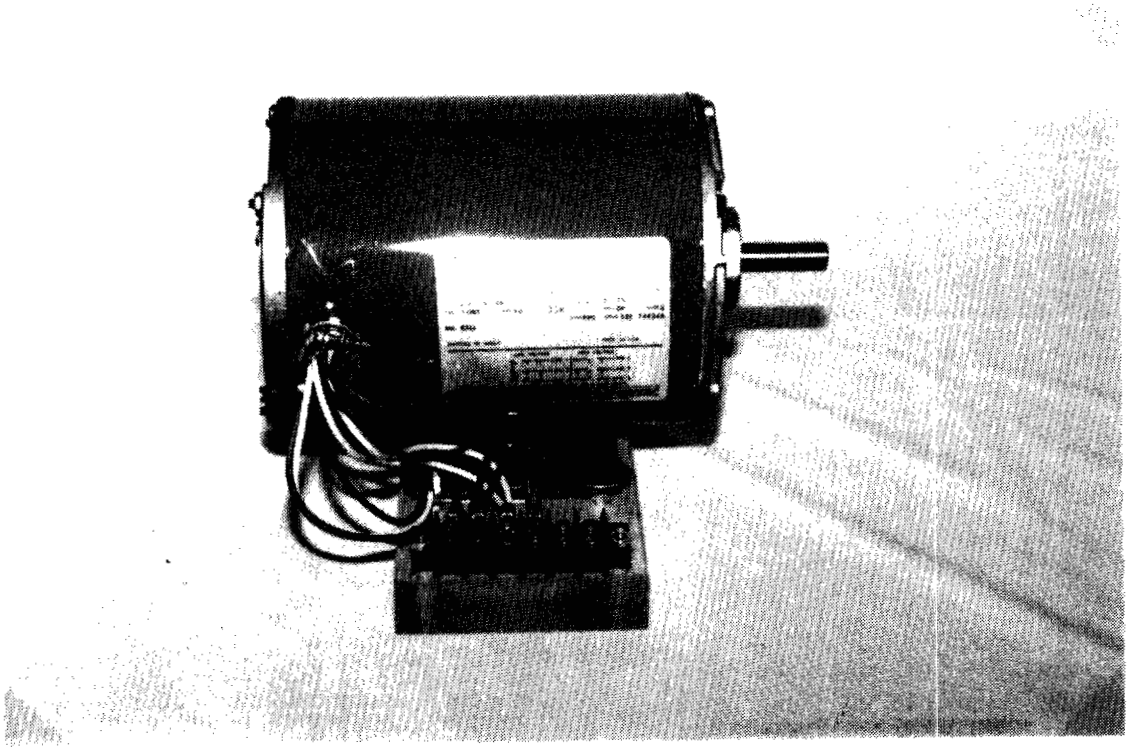

Figure 10 Test Motor Mounted on Plexiglas Base

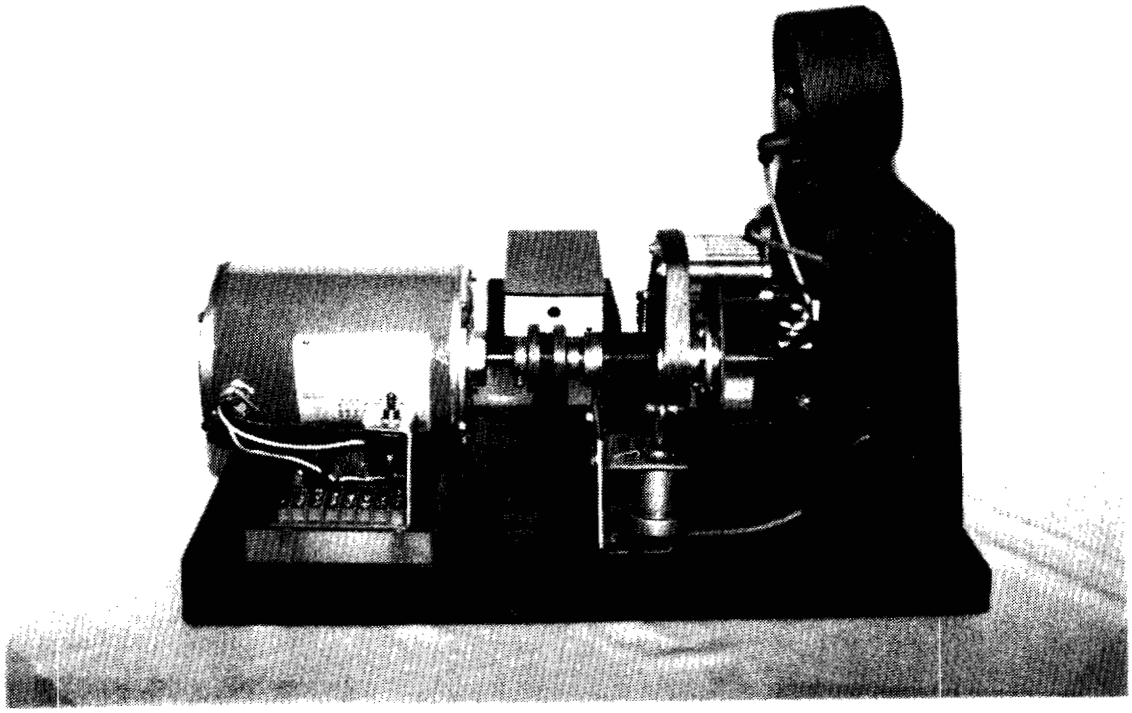

Figure 11 Plexiglas Mounted Test Motor and MAD Alignment

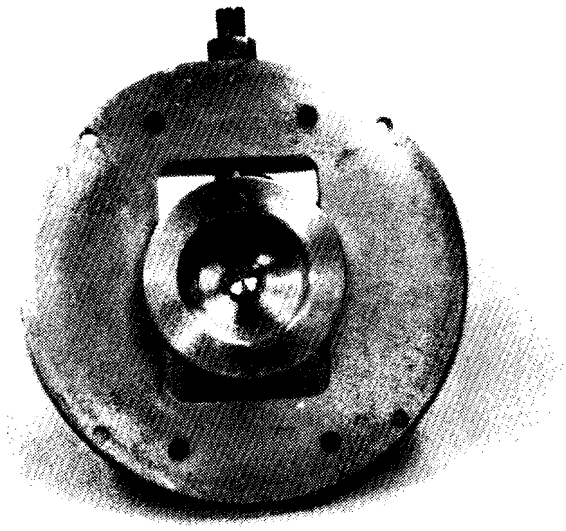

Figure 12 Inside View of Adjustable Bearing Carrier

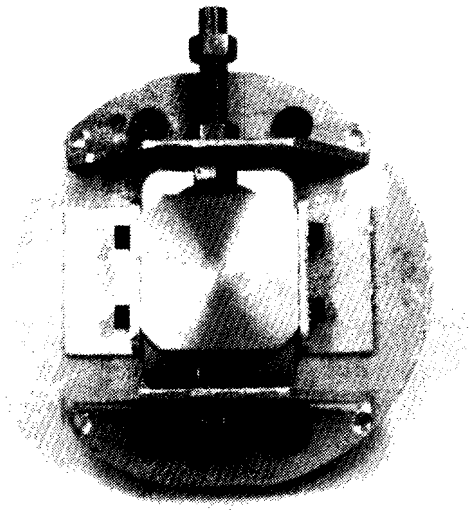

Figure 13 Outside View of Adjustable Bearing Carrier

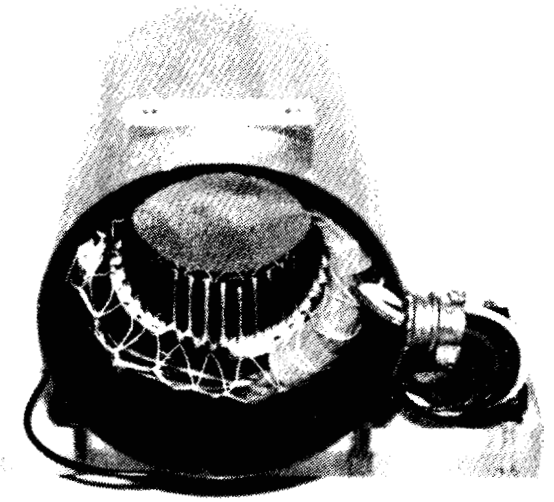

Figure 14 Test Machine Frame Modified for Depth Measurement

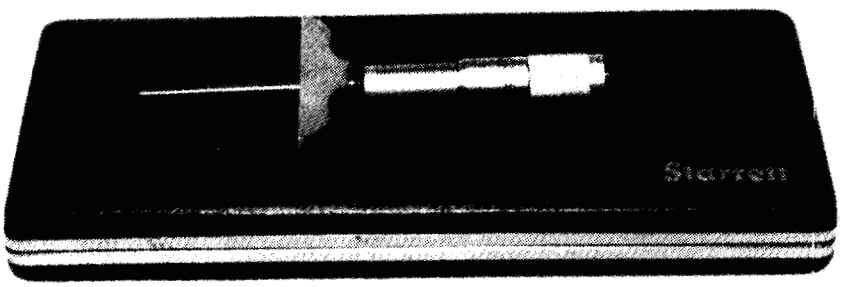

Figure 15 Depth Micrometer

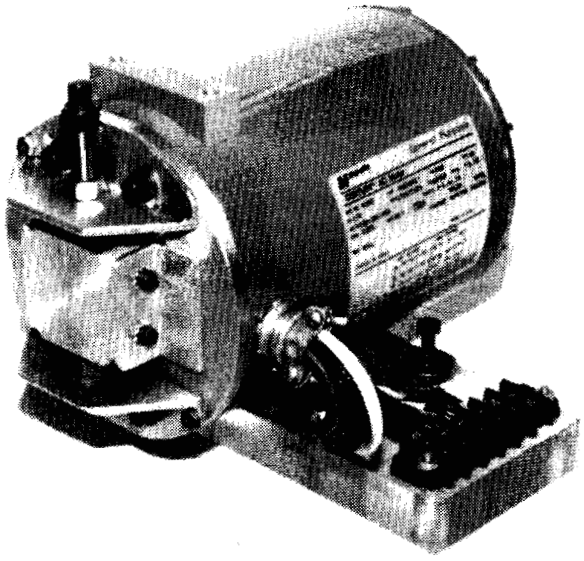

Figure 16 Side View of Assembled Rotor Eccentricity Test Motor

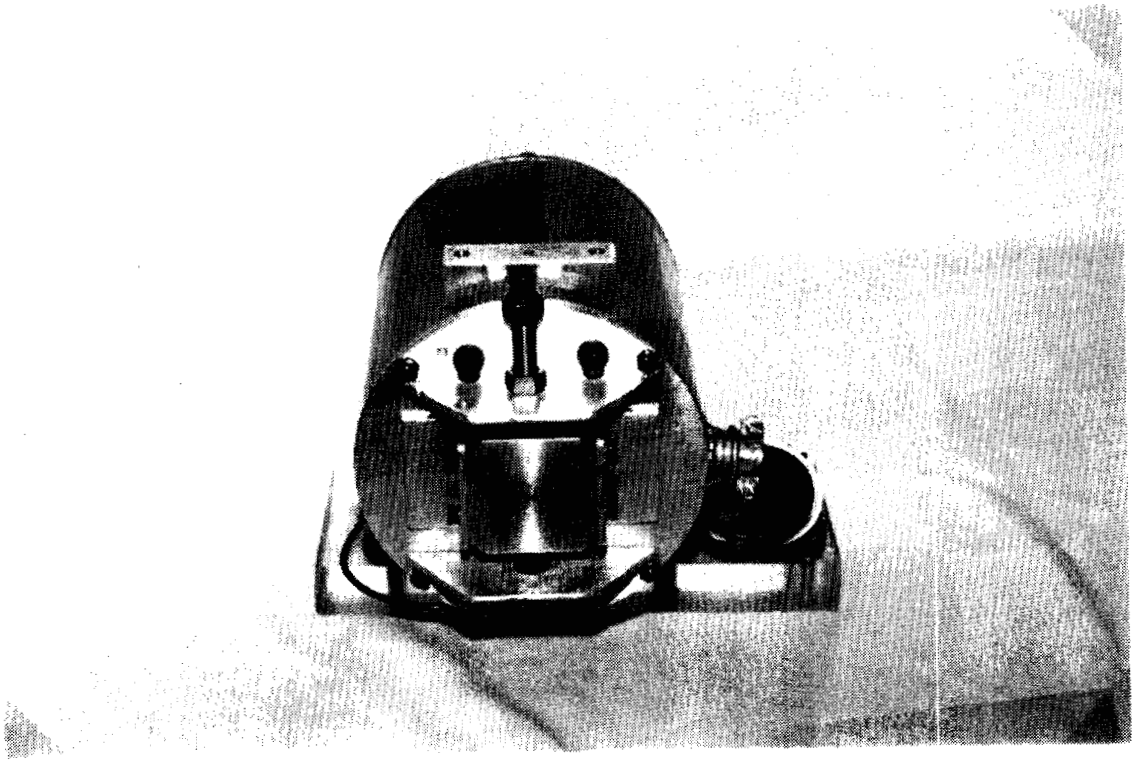

Figure 17 Front View of Assembled Rotor Eccentricity Test Motor

3.3.2 Stator Short and Open Circuit

Inserting the stator short and open circuit was a simple task with the machines used in this experiment. The stators in these machines were wound for either series or parallel connection. This allows the machines to be operated at either low or high voltage. Since the two coils of the stator windings were wired in parallel all that needed to be added was a center off, double pole, double throw switch. This switch would allow the motor to operate normally or faulted. In the short circuit mode one half of a stator phase coil would be shorted through a 20 ohm resistance. In the open circuit mode one half of the stator coil was opened. Figure 18 shows how the switch was mounted and wired. The only problem with this technique was that data had to be collected very quickly. With one half of a phase shorted or removed the other half of that phase will carry all the current supplied. This caused the motor to heat up very quickly. Using this technique for producing a stator fault did allow the motor to be switched back to its original form. Application of this method allowed multiple tests of the motor to be performed without permanent damage to the motor.

3.3.3 Rotor Broken Bar

The broken bar experiment was the last to be performed. There was no other course but to permanently damage the rotor. As can be seen in Figure 19, the rotor is a squirrel cage type with aluminum bars and end rings. After the base lint: run was performed and processed the motor was disassembled and one of the rotor bars was opened. This was performed with a 0.0625 inch milling tool that had been specially made for this purpose. With time and great care the aluminum in a small section of one bar was completely removed. The rotor bar of the test motor had a simple pear shape cross-section, making the removal of the material quite easy. The newly exposed faces of the rotor bar were resealed with several coats of polyurethane. This was done to provide a new layer of insulation over the bare metal. This experiment was performed with only one bar broken. It was not known at the time if having only one broken bar would create enough asymmetry in the rotor circuit to produce a detectable signal in the FFT output.

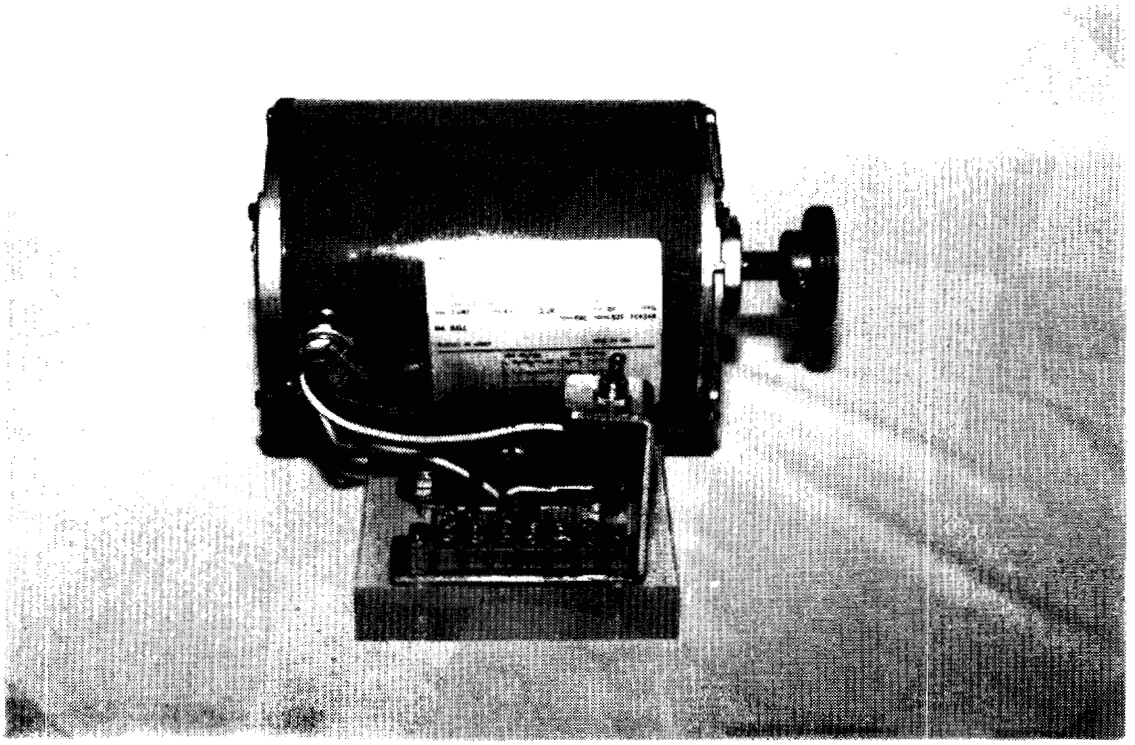

Figure 18 Stator Short and Open Circuit Test Motor Assembly

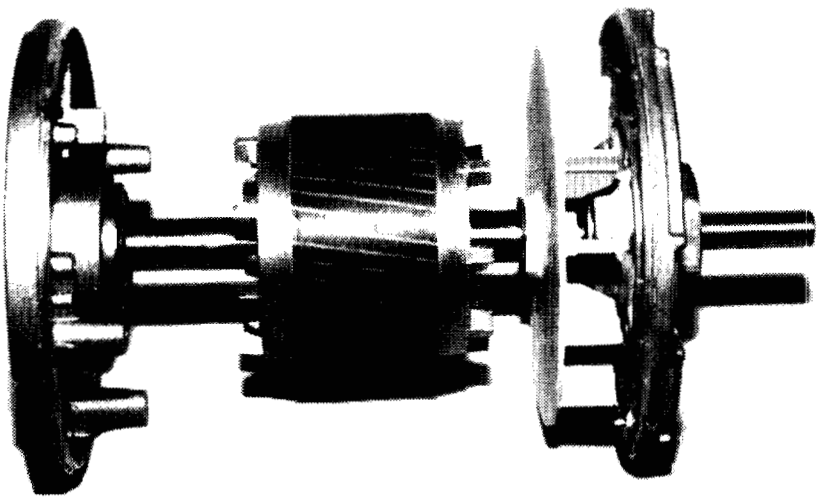

Figure 19 Squirrel Cage Rotor of the Test Motor

CHAPTER 4. EXPERIMENTAL RESULTS

4.1 Rotor Eccentricity

The machine eccentricity introduced in this experiment simulates that produced by a worn bearing. This particular type of eccentricity is static in nature, as compared to that produced by a flexible whirling rotor shaft, which is referred to as a dynamic eccentricity. For the static eccentricity in the first motor, Equation (2.1) in Chapter 2 describes the spatial harmonics produced. Table 1 shown below, was produced using this equation.

Table 1. Harmonic Frequencies Calculated for Rotor Eccentricity

Input Frequency	Motor Speed	Slip Developed	H.P. Developed
60 Hertz	1700 (R.P.M.)	0.055556	0.250

Integer k	M.M.F. (v)	Pos. Harmonic	Neg. Harmonic
1	1	1420.0	1300.0
1	3	1540.0	1180.0
1	5	1660.0	1060.0
1	7	1780.0	940.0
1	9	1900.0	820.0
1	11	2020.0	700.0
2	11	3380.0	2060.0
2	13	3500.0	1940.0
2	15	3620.0	1820.0
2	17	3740.0	1700.0
2	19	3860.0	1580.0
2	21	3980.0	1460.0
2	23	4100.0	1340.0
2	25	4220.0	1220.0
2	27	4340.0	1100.0

Table 1 has been modified to show only part of the list where the harmonic number of the stator m.m.f. time harmonics (v) of the theoretical equation varies from one to twenty seven in steps of two and the integer k is either one or two. These calculated harmonics were used to guide the search for actual fault harmonics. Although fault harmonics occurred throughout the FFT, this section of the data was specifically used due to the large number of fault harmonics occurring in one localized area. The next step in the process was to compare data collected on the test motor in both faulted and healthy conditions. Preprocessing of the data from the healthy and faulted conditions was completed and the FFT analysis was performed on both data files. Figure 20 and Figure 21 show the FFT analysis of the healthy and faulted motor data.

Comparison of these two graphs shows that the fault harmonics developed do not occur exactly at the calculated point. They also show that fault harmonics develop at points not even close to the calculated points. There are several explanations for these occurrences. First, the combination or mixing of fault harmonics with existing harmonics could cause the fault harmonic to shift from the calculated point. These pre-existing harmonics are due to the machine not being a perfect circuit. A comparison of the faulted and healthy motor graphs is performed so that these pre-existing harmonics may be identified. As seen at point one in the graphs, the magnitude increases and frequency is shifted closer to the calculated frequency of 1420 hertz. The increase in magnitude and frequency change are due to the fault harmonic. The fact that the fault harmonic does not fall at exactly 1420 hertz may be due to the effect that the base line harmonic (1) has on the fault harmonic. Point two shows a large increase in magnitude but is not one of the calculated fault harmonic frequencies. The harmonic shown at point three is developed with no initial harmonic at that point. This fault harmonic is not exactly at the calculated frequency of 1300 hertz but is close enough to cause concern of a developing fault. Point four shows a frequency shift and some magnitude loss from the base harmonic.

The second reason for possible error is due to human error. Although much time and care was taken in acquiring and processing the data, errors could occur in several places. For instance, the motor speed was read from the electronic tachometer when the data acquisition system was engaged. If the reading was off by even a small amount the frequencies calculated would be in error. Looking back to Chapter 2, Equation (2.1) uses slip to produce the theoretical fault harmonic frequencies. If the speed read from the electronic tachometer was in error by two R.P.M., the calculated fault harmonics

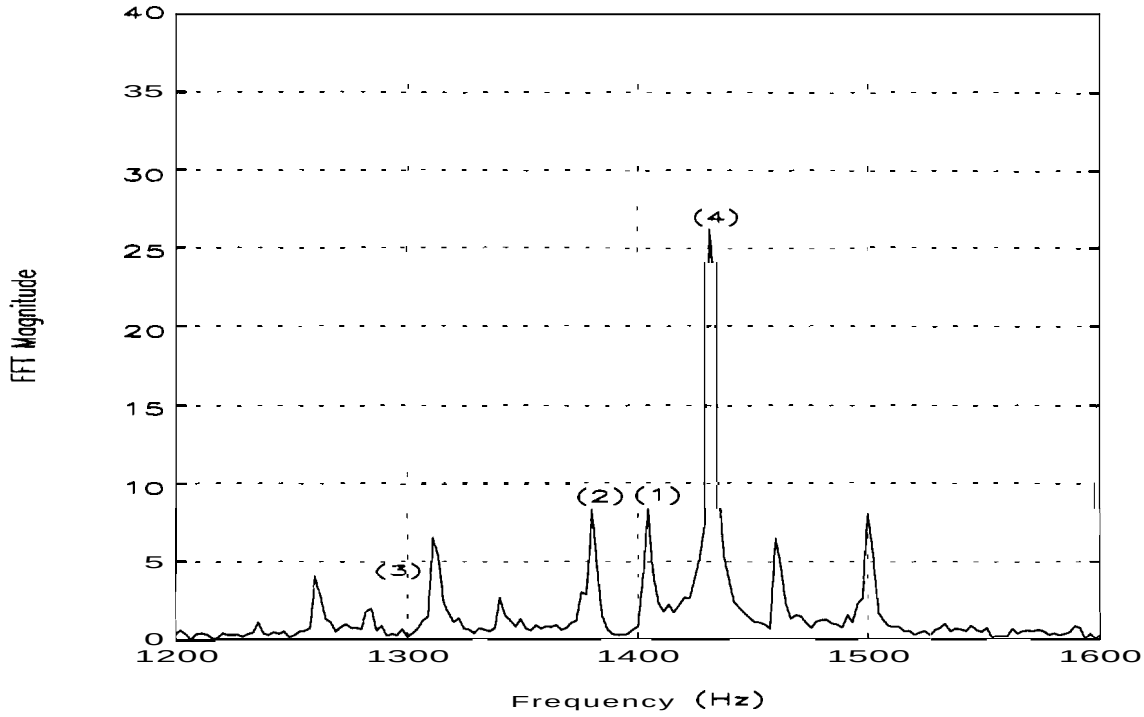

Figure 20 FFT Phase **A** Current: No Rotor Eccentricity

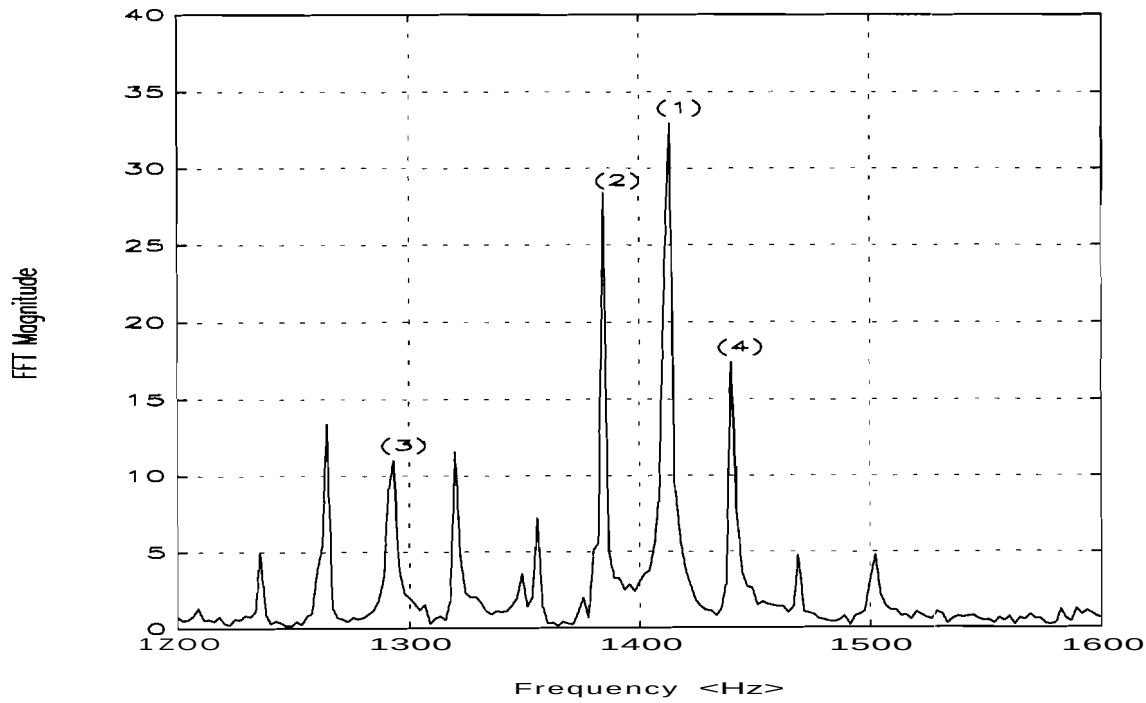

Figure 21 FFT Phase **A** Current: Rotor Eccentricity Fault

would be off by two hertz (using k=1 and v=3). If k and v were increased, say to three and five respectively, the frequency error would increase to five hertz. As can be seen in this example, the error will become larger as the fault harmonic frequency increases. This reading plays an important role in the fault calculation not only for the loading speed of the machine but the slip developed.

As stated earlier, and now shown in the comparison of the graphs, if the sampling frequency is not fast enough there could be a masking of harmonics by each other. A very narrow and sharp peak point on the harmonic plot is a good indicator that the peak was acquired. If the harmonic peaks are wide and do not come to a point a close by harmonic can be hidden in the plot. This does not mean that the data will not show a fault but using a faster sampling frequency could offer greater resolution to make the signature harmonic distinguishable from a close by harmonic.

4.2 Shorted and Opened Stator Winding

The second experiment was performed to simulate the short circuit and open circuit of one phase in the test motor. This process simply removed one half of the stator windings from the circuit, it was not a grounded short or complete loss of a phase. This was possible in the test motor due to the fact that each phase winding consisted of two coils wound in parallel. Only one half of the phase winding is shorted or opened thus allowing the motor to operate with all three phases. Using Equation (2.3) in Chapter 2 the fault calculation was performed with the proper speed and input frequency. Table 2 shows the calculated fault harmonic frequencies. A closer examination of Equation (2.3) shows there is no distinction between fault types. The same equation is used for calculating fault harmonics for both the shorted and open circuit faults. This lack of distinction between fault types raised some doubt as to the validity of Equation (2.3).

As before the next step was to process the acquired data on the healthy and faulted motor files and perform the FFT's. Since fault harmonics are not confined to a specific range of frequencies the whole FFT spectrum had to be analyzed. This involved a plot by plot comparison of the FFT's keeping in mind the calculated fault frequencies. Several of the articles read [1, 3, 7] referred to the "Zoom FFT" for processing the data. This would allow smaller ranges of the FFT plots while holding the FFT accuracy. The mathematical based program used in this experiment was not fitted with a "Zoom FFT" option. To overcome this obstacle, the sampling frequency was raised so that when the plot ranges were modified the resolution of the plots was not

affected. Modifying the ranges to a portion of the original, allowed for the comparisons to be performed on the data in smaller sections. Sectioning of the FFT allowed the operator to pin point areas of interest.

Table 2. Harmonic Frequencies Calculated for a Stator Fault

Input Frequency	Motor Speed	Slip Developed	H.P. Developed
60 Hertz	1700 (R.P.M.)	0.055556	0.248

M.M.F. (v)	Pos. Harmonic	Neg. Harmonic
1	3.3	116.0
3	130.0	230.0
5	256.7	343.0
7	383.3	456.6
9	510.0	570.0
11	636.7	683.3
13	763.3	796.7
15	890.0	910.0
17	1016.7	1023.3
19	1143.3	1136.7
21	1270.0	1250.0
23	1396.7	1363.3
25	1523.3	1476.7
27	1650.0	1590.0
29	1776.7	1703.3
31	1903.3	1816.7

4.2.1 Short Circuit Stator Winding

The short circuit FFT plots were compared and the results were much like those of the rotor eccentricity. There were fault harmonics developed at frequencies where harmonics already exist, frequency shifting of some harmonics closer to the fault harmonic frequency calculated, loss of healthy motor harmonics, and fault harmonics developing at frequencies not calculated by Equation (2.3). Figure 22 and Figure 23 were chosen to represent the healthy and faulted motor data due to all of these different types of harmonics in one localized area.

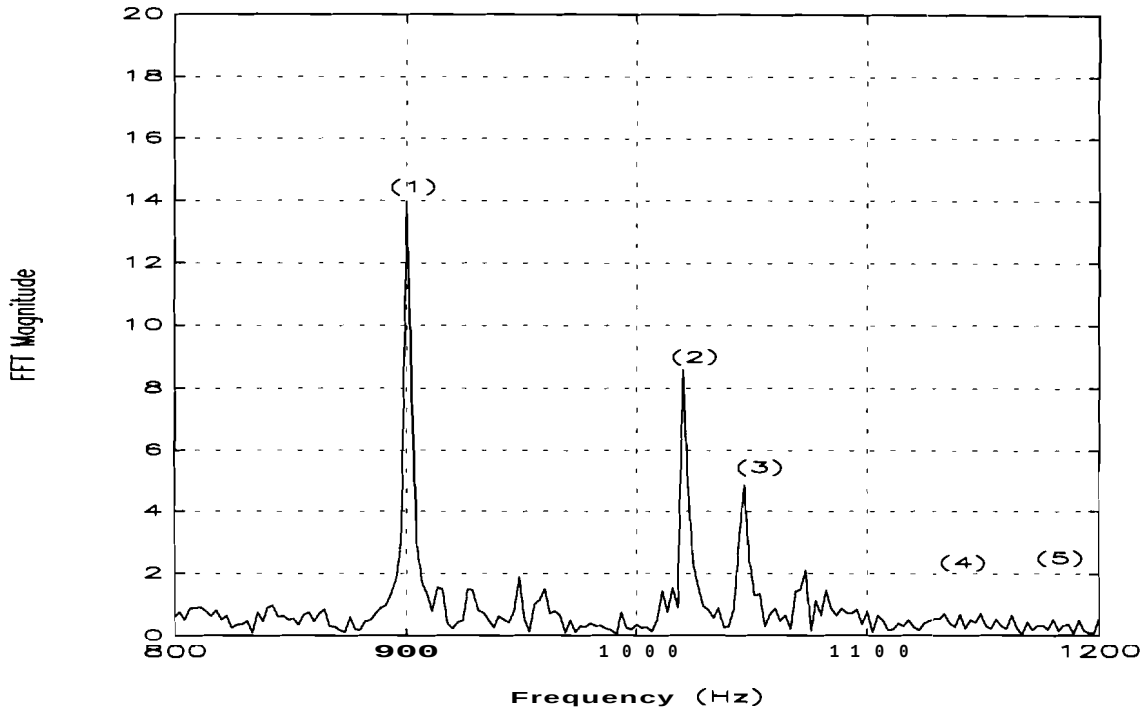

Figure 22 FFT Phase B Current: No Stator Fault

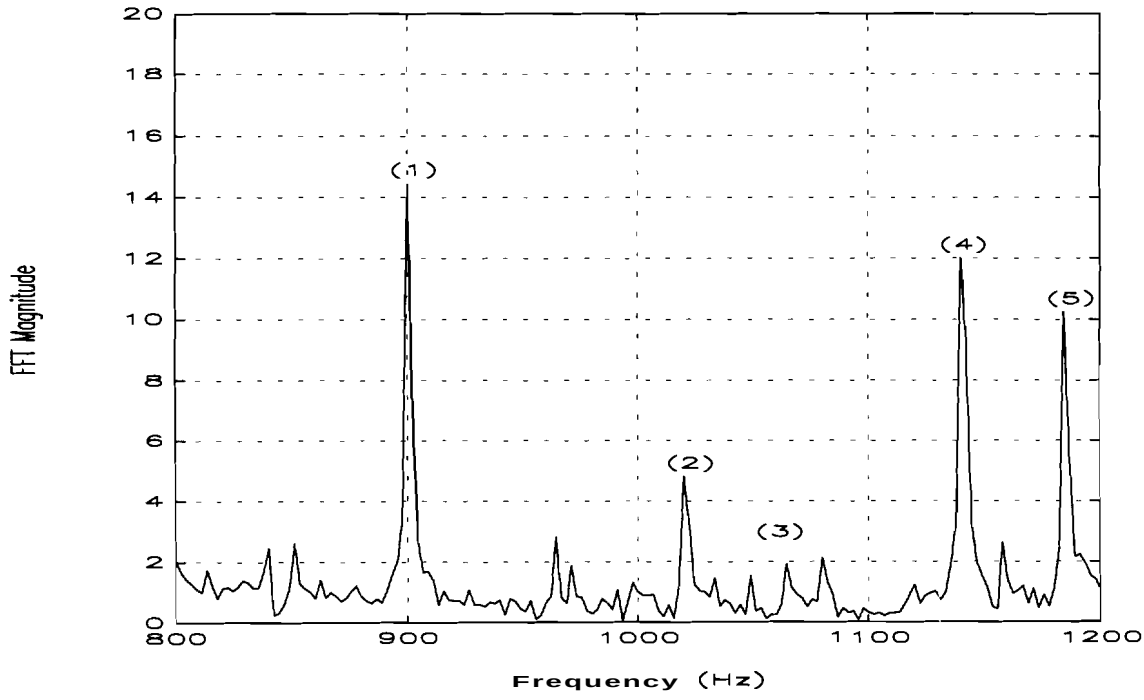

Figure 23 FFT Phase B Current: Stator Short Circuit Fault

As observed in the graphs point one has increased very little in magnitude and the: base of the harmonic has not widened. This leads to the conclusion that the calculated fault harmonic for this area did not develop. Point two shows a large magnitude decrease with no apparent frequency shift and is close to the calculated frequency of 1023 hertz. Point three shows the loss of the base harmonic in the faulted harmonic data. This could simply be due to the changes made to the stator circuit. It does though show that some change has occurred. Points four and five are the most interesting of these two graphs. Both of these fault harmonics arise from no previous harmonic in the healthy data. Point four is located exactly at the calculated fault harmonic frequency of 1143.3 hertz. There is not even a small signal in the healthy base harmonic data. The magnitude and width of this fault harmonics base leads to the conclusion that this is a very strong asymmetry signal. From Table 2, it can be seen that there are no fault harmonics calculated for the area where point five is located. Observations of the next higher range of plots did not show any base harmonic that may have been shifted to this frequency. As in the rotor eccentricity experiment, this fault harmonic just developed.

4.2.2 Open Circuit Stator Winding

Comparison of the open circuit sets of FFT's proved to be almost useless. Other than a small loss in magnitude at some frequencies and a small shift in some of the harmonics frequencies there were no changes between the faulted and healthy data. This leads to the conclusion that loss of part of a stator winding will not be shown in the input current as predicted. The magnitude change could be expected by the resistance change in the faulted stator phase. Figure 24 and Figure 25 show this loss in magnitude in the FFT's. Also seen in these figures is a frequency shift of the number three harmonic from 1045 hertz to 1060 hertz and a small spike that has become visible at 1027 hertz. Due to the base width of harmonic three in the healthy state, it is unclear if a fault harmonic has developed or if a previously aliased base harmonic has been allowed to stand out. It is possible that the small spike was previously combined with the harmonic at 1060 hertz to form the harmonic at 1045 hertz in the unfaulted data. The resistance change also caused the input current level to decrease. As can be seen in Figure 26 and Figure 27, the magnitude of the faulted motor input current is much lower than the input current of the healthy motor. These two figures also show a very noticeable distortion of the input current waveform. At first it was hoped this distortion

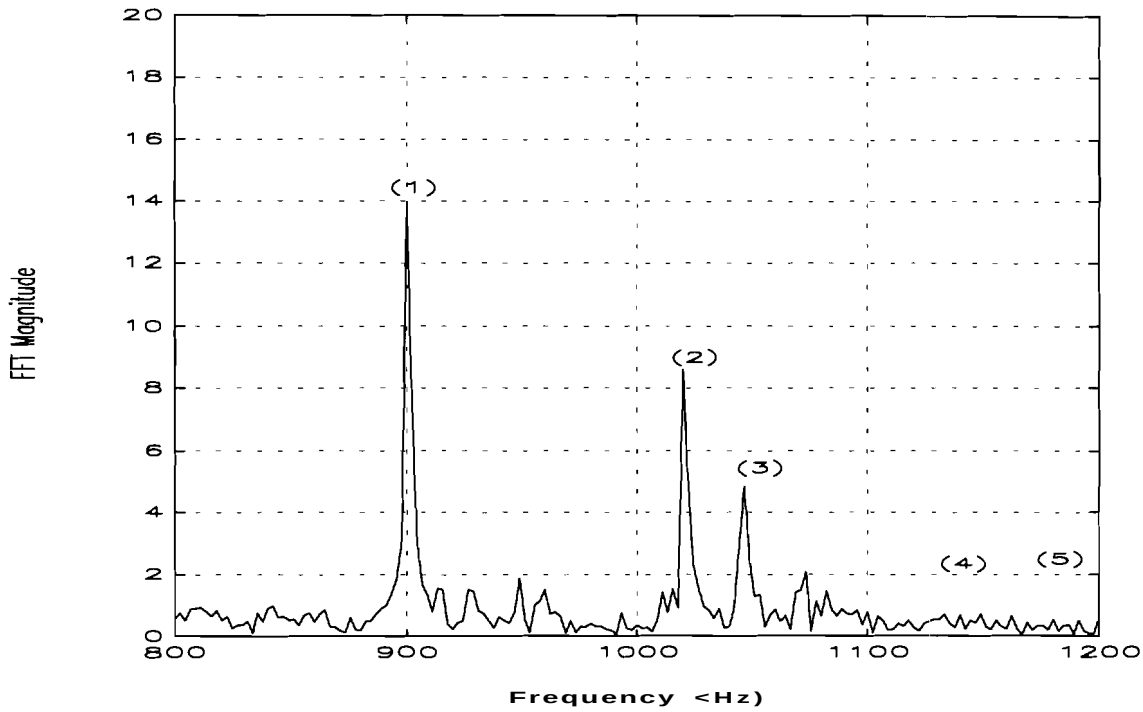

Figure 24 FFT Phase B Current: No Stator Fault

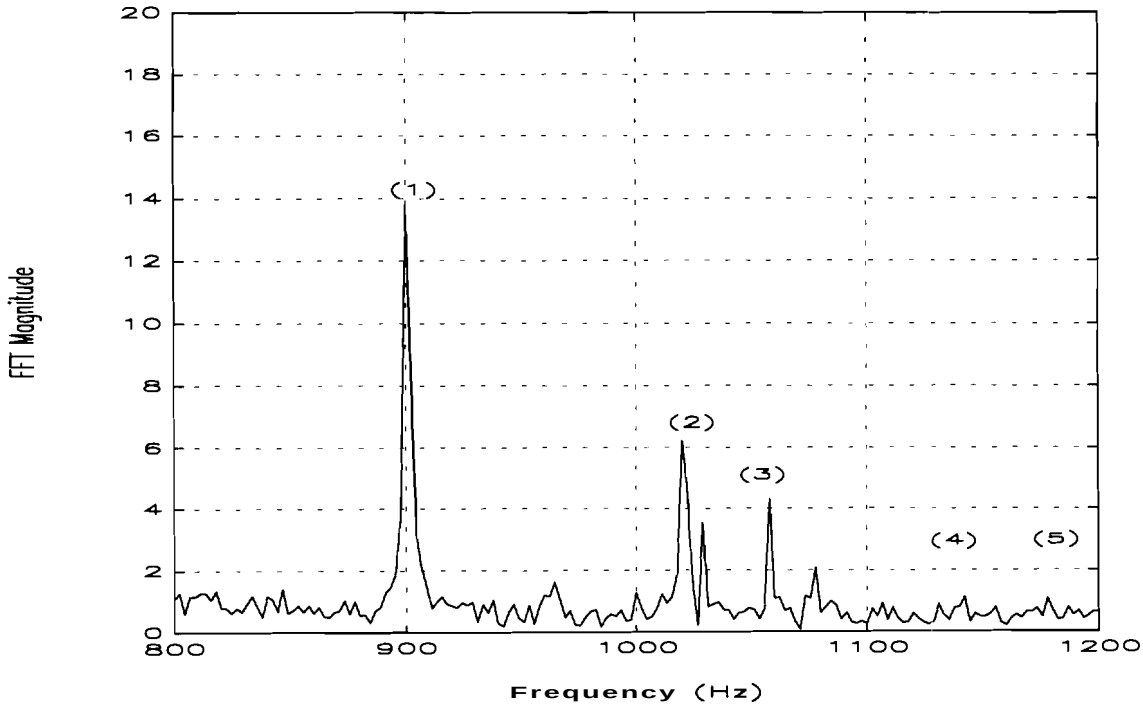

Figure 25 FFT Phase B Current: Stator Open Circuit Fault

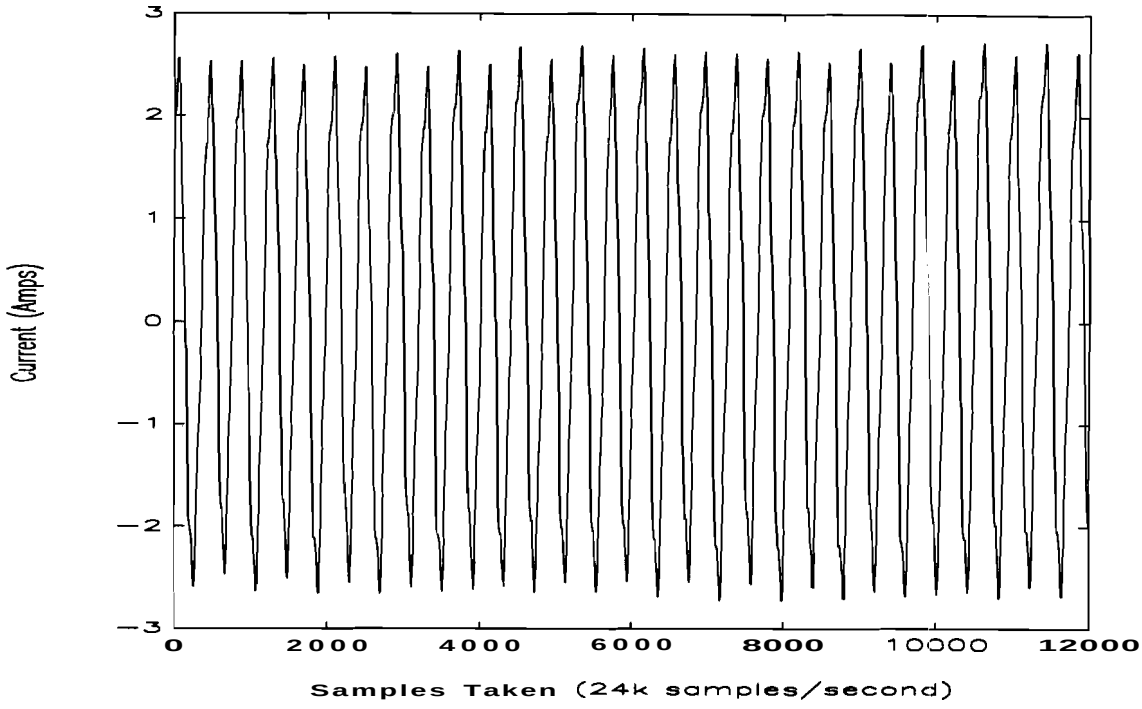

Figure 26 Phase B Current Data: No Stator Fault

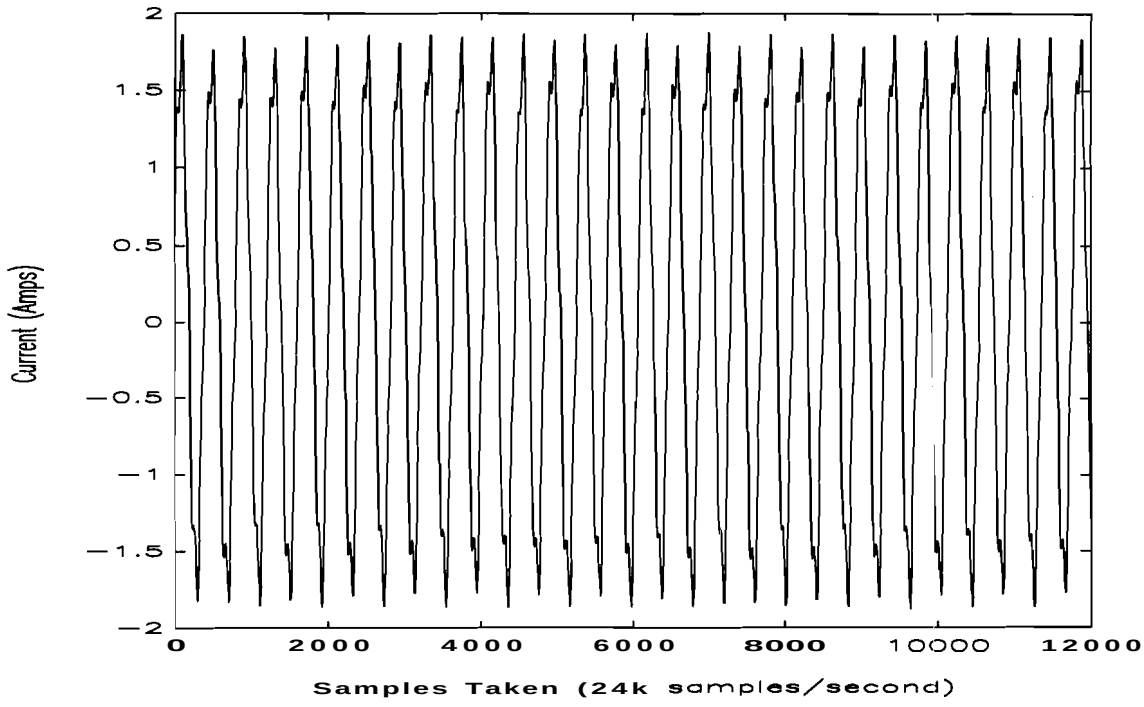

Figure 27 Phase B Current Data: Stator Open Circuit Fault

would produce some definite harmonics but after processing the FFT's these expected harmonics were never found.

The loss of magnitude may also be explained by the way that the motors were produced. It is not known (proprietary information) if the two windings were overlaid in exactly the same winding pattern. If the two sets of windings were overlaid exactly then the base harmonics produced would be alike. A loss of one half of the phase winding would not change the base pattern it would just reduce the magnitude of the pattern. The two windings would still be magnetically coupled thus no real change would have occurred in the motor.

It was thought that the predicted harmonics may not show up in the faulted phase input current but in one of the other inputs. The comparison process was repeated for the other lines. There were no changes between the healthy and faulted data other than the magnitude drops were not present. This fact gives relevance to the idea that the magnitude drop is due to the change in resistance of the faulted phase and not to some harmonic component.

A side note which has been considered but is not part of this experiment, is the fact that the collected data could be used to calculate the instantaneous power [11]. This power calculation could be used to show a change in the motor. Equation (4.1) shows that the distorted input current could have a large effect on the instantaneous power of the motor.

$$p_{ab} = v_{ab}(t)^* \bullet i_{ab}(t) \qquad \ldots (4.1)$$

The distortion and magnitude loss in the input currents are very obvious. With proper experimentation and analysis this technique could be used to link a particular fault with specific readings. Using this information could prove to be very beneficial in future experimentation.

4.3 Broken Bar

The final machine fault was quite simple to initiate. Unfortunately, it permanently damaged the test machine. For this reason several runs were made so that data on the healthy machine could be acquired and stored. The test machine was then faulted and the same data collection techniques were used to collect faulted data. As stated before only one bar was broken in this experiment. As can be seen in the theoretical calculation, Equation (2.4) of Chapter 2, the number of broken bars seems to

have no effect on the harmonics calculated. Another interesting observation was made about Equation (2.4). The fact that the number of rotor bars present or the amount of rotor bar skew is not taken into consideration when calculating rotor fault harmonics. Using the known components of motor speed and base input frequency, Table 3 was produced.

This table of calculated fault harmonics shows several frequencies close to the base input frequency of 60 hertz. This was not evident in the earlier experiments. The other fault harmonics calculated for this experiment seem to be evenly distributed through out the spectrum. References used for this experiment [1, 7, 9] paid special attention to the area around the base input frequency when performing their analysis with a spectrum analyzer. For these reasons special interest was also given to the area surrounding the base input frequency in this experiment. The FFT analysis were performed on the acquired data and the comparison of these FFT's completed.

Table 3. Harmonic Frequencies Calculated for Broken Bar Faults

Input Frequency	Motor Speed	Slip Developed	H.P. Developed
60 Hertz	1700 (R.P.M.)	0.055556	0.245

M.M.F. (v)	Pos. Harmonic	Neg. Harmonic
1	60.0	53.3
3	173.3	166.7
5	286.7	280.0
7	400.0	393.3
9	513.3	506.7
11	626.7	620.0
13	740.0	733.3
15	853.3	846.7
17	966.7	960.0
19	1080.0	1073.3
21	1193.3	1186.7
23	1306.7	1300.0
25	1420.0	1413.3
27	1533.3	1526.7
29	1646.7	1640.0

As can be seen in Figure 28 and Figure 29 a definite peak has developed at 53 hertz. In reference to earlier statements, the base frequency harmonic peak has widened thus partially hiding the harmonic developed. A magnification of this area, Figure 30 and Figure 31, show that harmonics have developed at 280 hertz and 385 hertz. The latter is not located exactly on the calculated frequency. This shift may be due to the strength of other harmonics in the area or may be caused by the multiplying of any error at higher frequencies. If, for instance, the speed of the machine was changing during the collection of data, the effects would be much greater at high frequencies than at low frequencies.

Further comparison of the data shows fault harmonics developing throughout the spectrum. Not all calculated harmonics did develop and some fault harmonics developed at frequencies not calculated. As before there were disappearances of existing harmonics in areas were fault harmonics were supposed to be found. It was observed that fault harmonics at higher frequencies were shifted somewhat. They were not as exact as the harmonics at lower frequencies. This gives relevance to the idea that the error grows as the frequency increases. Although fault harmonics were observed at higher frequencies, the plots of the lower frequencies still provided the best analysis.

As stated previously, skew may have some effect on the fault harmonics developed. The skewing of rotor bars is designed to reduce the effects of space harmonics in the air-gap flux density [12]. With rotor skew, the direction of the current in a rotor bar is no longer axial, but has a peripheral component proportional to the sine of the angle of skew. It is possible that the skewing could also mask out some of the signature harmonic components associated with a broken rotor bar.

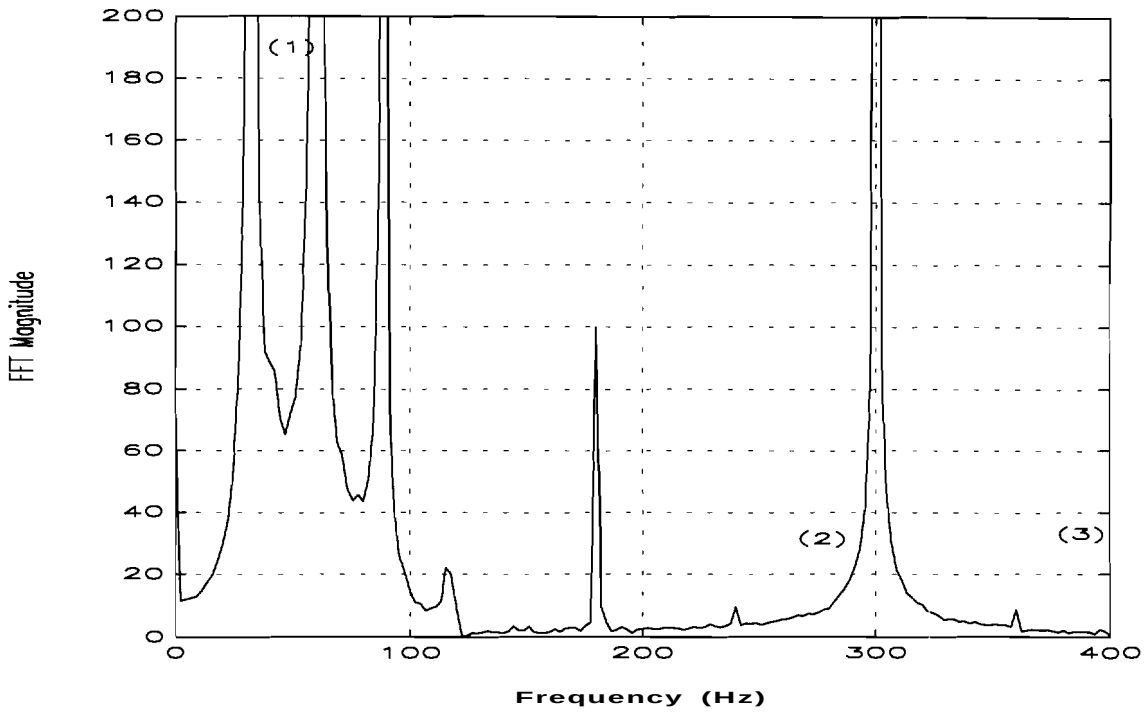

Figure 28 FFT Phase A Current: No Broken Bar Fault

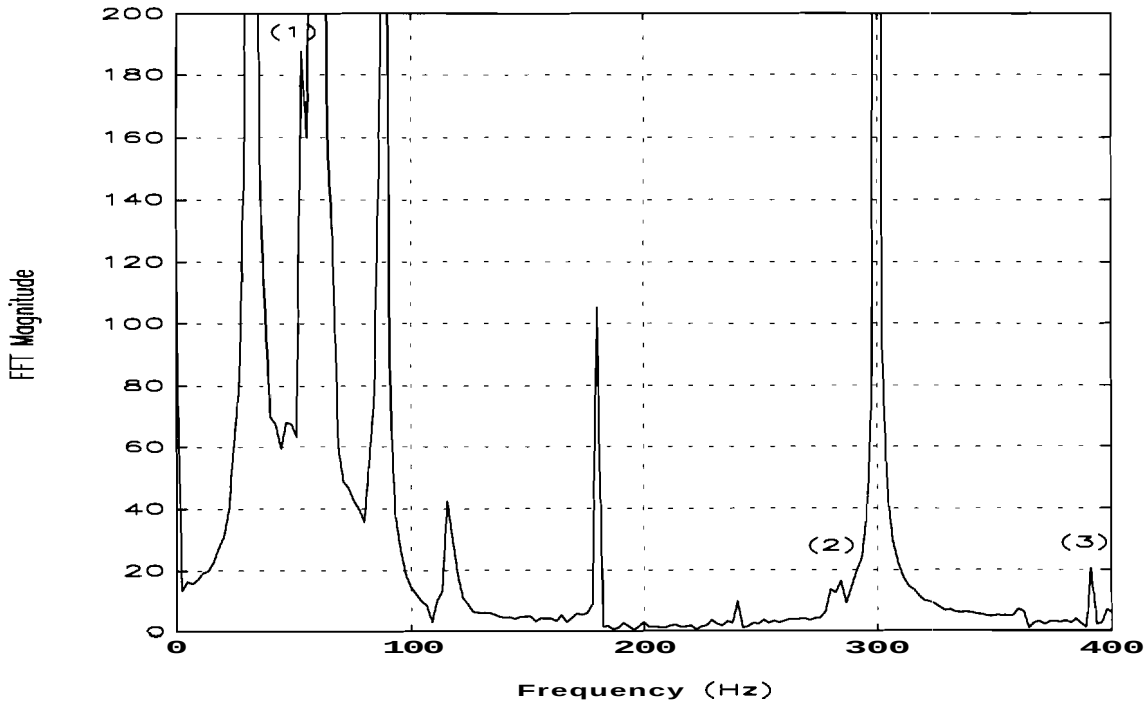

Figure 29 FFT Phase A Current: Broken Bar Fault

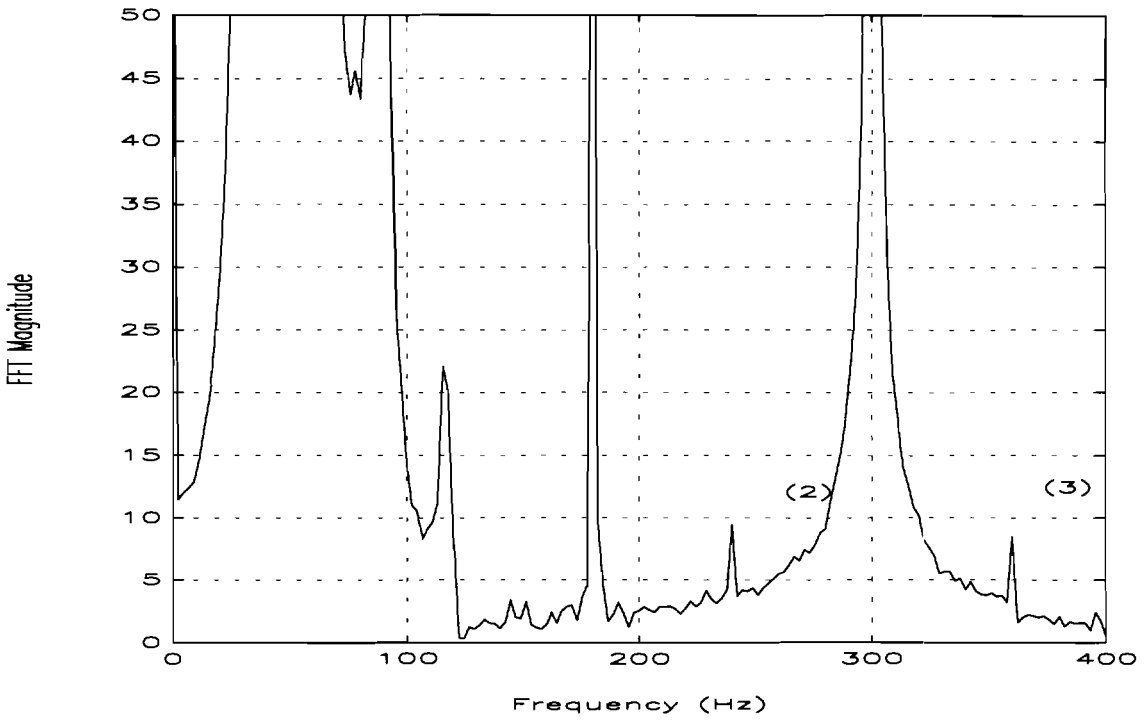

Figure 30 FFT Phase A Current: No Broken Bar Fault

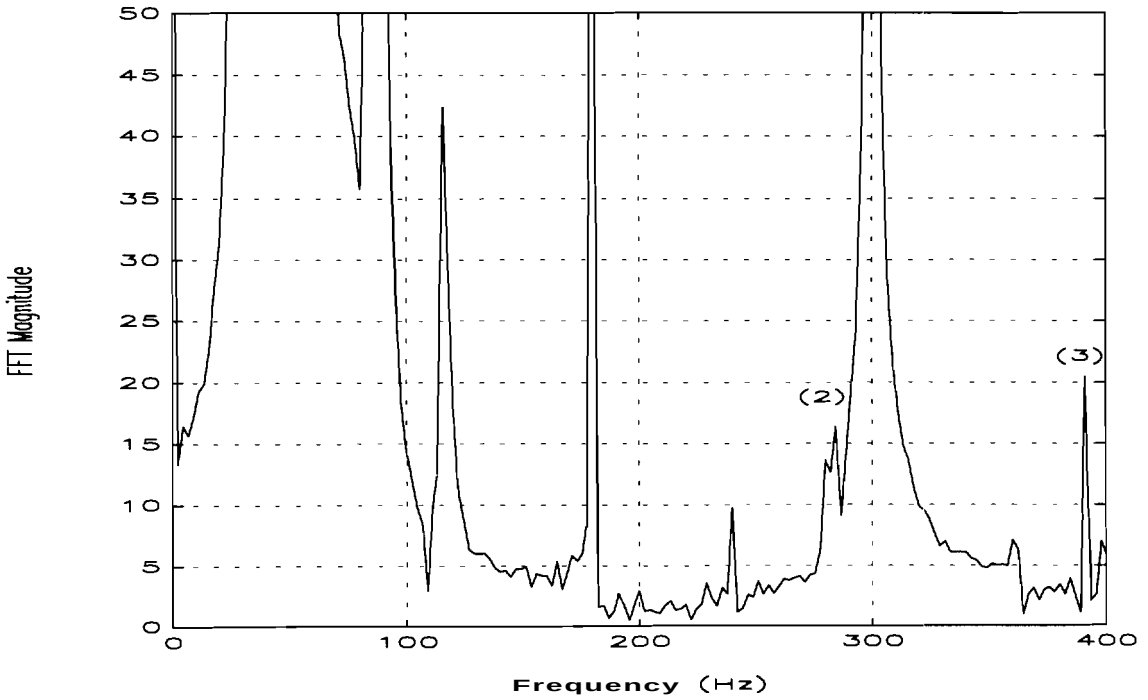

Figure 31 FFT Phase A Current: Broken Bar Fault

CHAPTER 5. CONCLUDING REMARKS

5.1 Summary

This project was implemented with two objectives in mind: 1) investigate the efficiency of existing methods for on-line fault detection when applied to three-phase induction motors; and 2) provide a foundation for future research in this area. The basis of how fault harmonics develop has been explained in this present work. These ideas and the theoretical equations to calculate fault harmonics have been tested and the experimental results have supported the theoretical analysis.

There are certain precautions which should be taken during experimentation and data processing. Great care should be taken during the acquisition of the data so that errors are not introduced into the experiment. It was shown that even when precautions were taken some types of errors were still possible. In the future it may be possible to automate the acquisition system so that these types of errors will not happen. Special equipment was developed to produce the motor faults needed for this experimentation and the experimenter must be aware of how this equipment was intended to operate. During data processing, errors due to spectral leakage can be reduced using standard windowing techniques on the signal data acquired. Plotting of the processed data in the form of FFT plots needs special attention. As discussed in Chapter 3, the frequency calculated for the FFT plot may include a small drift in the fundamental frequency that can be easily overlooked.

Using all the precautions mentioned in this work will allow the operator to obtain accurate results from the FFT analysis on the current data acquired. Comparing the tabulated data from the fault harmonic calculations and the FFT plots produced, a technician may determine whether a fault exists in an induction motor and what type.

5.2. Recommendations

As was discussed in Chapter 1, there is growing interest in fault diagnostics by inclustry. Many industrial applications warrant monitoring of critical motors so that expensive equipment and delicate processes are not interrupted or damaged. With this in mind, the need for further research in the area of motor fault diagnostics is

imperative. The basic theory is well documented for induction motor faults. Work needs to be done to expand the theory to other types of motors and to simplify the present laboratory equipment. With advances in instrumentation and processors, moving the identification technique from the laboratory to the factory floor should be possible in the near future. Emphasis has to be made in producing equipment that is simple to operate and cost effective.

Another area that needs to be addressed is that of merging other types of fault diagnostics with input current analysis. For example, if vibration analysis were used as a cross check, pin pointing a specific type of fault would be easier. Presently, a worker has different equipment performing different types of tests. In the future, if one piece of equipment were capable of performing several different tests, the technician or repairman could easily monitor critical equipment, thus reducing down time and repair costs.

BIBLIOGRAPHY

BIBLIOGRAPHY

[1] P. Vas, "Parameter Estimation, Condition Monitoring, and Diagnosis of Electrical Machines", Clarendon Press, Oxford, 1993.

[2] S. Elder, J. F. Watson, W. T. Thomson, "Fault Detection in Induction Motors as a Result of Transient Analysis", 4th International Conference on Electrical Machines and Drives, Vol. 310, pp. 182-186, Sept. 1989.

[3] J. R. Cameron, W. T. Thomson, A. B. Dow, "Vibration and Current Monitoring for Detecting Airgap Eccentricity in Large Induction Motors", IEE Proceedings, Vol. 133, Pt. B, No. 3, pp. 155-163, May 1986.

[4] J. R. Cameron, W. T. Thomson, A. B. Dow, "On-Line Current Monitoring of Induction Motors-A Method for Calculating the Level of Airgap Eccentricity", Proceedings IEE Conference on Electrical Machines - Design and Applications, No 282, pp. 173-178, 1987.

[5] S. L. Ho, "Condition Monitoring of Induction Motors", 5th International Conference on Electrical Machines and Drives, Vol. 341, pp. 56-60, Sept. 1991.

[6] J. Penman, P. J. Tavner, "Condition Monitoring of Electrical Machines", Wiley & Sons, New York, 1987.

[7] G. B. Kliman, J. Stein, "Methods of Motor Current Signature Analysis", Electric Machines and Power Systems, Vol. 20, No. 5, pp. 463-4.74, Sept-Oct. 1992.

[8] S. J. Yang, "Low Noise Electric Motors", IEE Monographs in Electrical and Electronic Engineering, Oxford Science Publications, 1981.

[9] W. T. Thomson, I. D. Stewart, "On-Line Current Monitoring for Detecting Airgap Eccentricity and Broken Rotor Bars in Inverter Variable Speed Drives", International Conference on Electrical Machines, pp. 211-214, Sept. 1988.

[10] K. G. Beauchamp, "Signal Processing - Using Analog and Digital Techniques", George Allen & Unwin Ltd., London 1973.

[11] R. Maier, "Protection of Squirrel-Cage Induction Motor Utilizing Instantaneous Power and Phase Information", IEEE Transactions on Industry Applications, Vol. 28, No. 2, pp. 376-380, March/April 1992.

[12] M. G. Say, "Alternating Current Machines", A Halsted Press Book, John Wiley & Sons, New York 1983.